Research Square

Preprints are preliminary reports that have not undergone peer review.
They should not be considered conclusive, used to inform clinical practice,
or referenced by the media as validated information.

Quality-by-design development of folic acid–engineered berberine nanoliposomes for targeted triple-negative breast cancer therapy

Roshni Singh
Delhi Pharmaceutical Science and Research University
Debopriya Dutta
Delhi Pharmaceutical Science and Research University
Namrata Gautam
Delhi Pharmaceutical Science and Research University
Meenakshi Tanwar
inderprastha engineering college
Karishma Niveria
University of Delhi
Disha Mittal
University of Delhi
Anita Kamra Verma
inderprastha engineering college
Surajita Sahu
National Institute of Technology Rourkela
Saurabh Mittal
saurabhmittal904@gmail.com

Amity University
Sushama Talegaonkar
Delhi Pharmaceutical Science and Research University

Research Article

Keywords: Berberine, Folate receptor targeting, Oxidative stress, Targeted drug delivery, Triple-negative breast cancer

Posted Date: June 17th, 2026

DOI: https://doi.org/10.21203/rs.3.rs-9657254/v1

License: This work is licensed under a Creative Commons Attribution 4.0 International License.
Read Full License

Additional Declarations: No competing interests reported.

Quality-by-design development of folic acid–engineered berberine nanoliposomes for targeted triple-negative breast cancer therapy

Roshni Singh[1], Debopriya Dutta[1], Namrata Gautam[1], Meenakshi Tanwar[2], Karishma Niveria[3], Disha Mittal[3,4], Anita Kamra Verma[2,5], Surajita Sahu[6], Monalisa Mishra[6], Saurabh Mittal[7*], Sushama Talegaonkar[1*]

[1]Department of Pharmaceutics, School of Pharmaceutical Sciences, Delhi Pharmaceutical Sciences and Research University, New Delhi, India

[2]Inderprastha Engineering College, Ghaziabad, India

[3]Nanobiotech lab, Kirori Mal College, University of Delhi, Delhi, India.

[4]Department of Life Sciences, School of Biosciences and technology, Galgotias University, Greater Noida, U.P, India

[5]Fellow, Delhi School of Public Health, Institution of Eminence, University of Delhi, Dehi-110007., India

[6]Neural Development Biology Lab, Department of Life Science, NIT Rourkela, Rourkela, Odisha, India

[7]Department of Pharmaceutics, Amity Institute of Pharmacy, Amity University, Noida - 201303, U.P., India

[*]**Author for Correspondence:**

Corresponding author: Dr. Sushama Talegaonkar

Department of Pharmaceutics, School of Pharmaceutical Sciences, Delhi Pharmaceutical Sciences and Research University, New Delhi, India

Email: stalegaonkar@dpsru.edu.in

Mobile No.: +91-9818453518

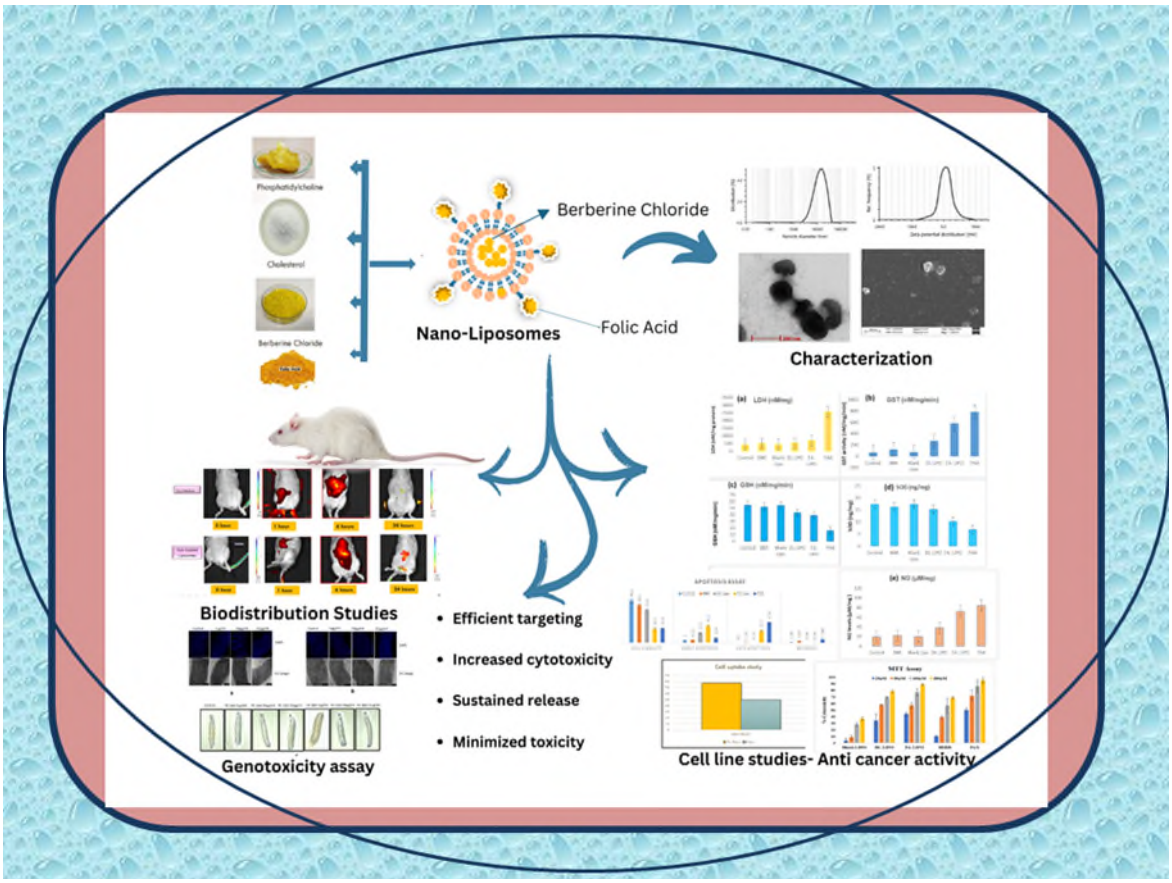
Co-Corresponding author: Dr. Saurabh Mittal

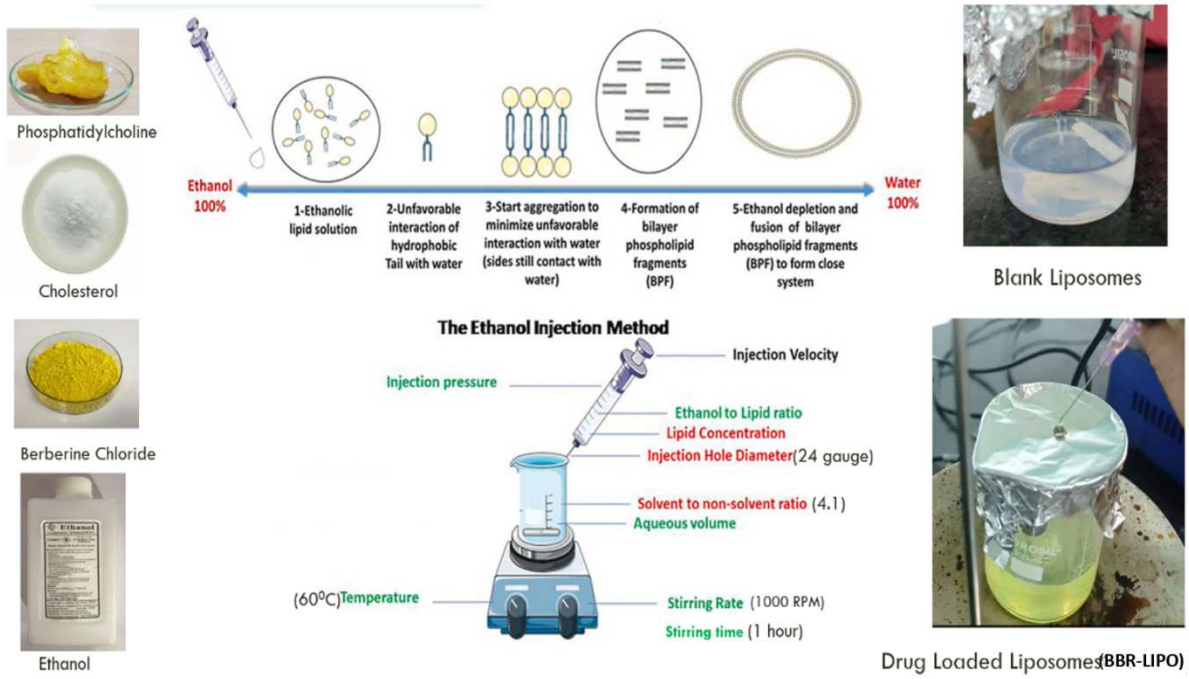
Department of Pharmaceutics, Amity Institute of Pharmacy, Amity University, Noida - 201303, U.P., India

E-mail: saurabhmittal904@gmail.com

Mobile No.: +91-9560912817

Graphical Abstract





Synthesis of BBR-nanoliposomes by ethanol injection

Abstract

Triple-negative breast cancer (TNBC) remains one of the most challenging breast cancer subtypes due to the lack of actionable molecular targets and the systemic toxicity associated with standard chemotherapy. Berberine chloride (BBR), a plant-derived isoquinoline alkaloid, exhibits promising anticancer activity; however, its poor solubility and limited bioavailability restrict therapeutic utility. In this study, folic acid–decorated nanoliposomes were developed to enhance the targeted delivery of BBR to TNBC cells. BBR-loaded liposomes and folic acid–functionalized liposomes were prepared using the solvent injection method and optimized through a Quality-by-Design (QbD) framework. The optimized folate-modified formulation showed a mean particle size of 168.3 nm with an entrapment efficiency of 41.8%, while non-targeted liposomes exhibited a smaller size (95.6 nm) and slightly higher drug loading (47.5%). Both systems provided sustained drug release over 72 hours, with folate-decorated liposomes demonstrating a more controlled release pattern. Cytotoxicity studies in MDA-MB-231 cells revealed significantly enhanced antiproliferative activity of folate-functionalized nanoliposomes (IC_{50} = 24.72 μM) compared to non-targeted liposomes and free BBR. Increased intracellular reactive oxygen species generation following folate-mediated delivery suggested oxidative stress–driven cell death as a contributing mechanism. Importantly, genotoxicity evaluation using *Drosophila melanogaster* confirmed the safety of the liposomal formulations. Overall, folic acid–decorated nanoliposomes substantially improve the therapeutic efficacy of berberine and offer a rational, targeted nanocarrier approach for TNBC management.

Keywords: Berberine; Folate receptor targeting; Oxidative stress; Targeted drug delivery; Triple-negative breast cancer

1. Introduction

Triple-negative breast cancer (TNBC) is an aggressive subtype, accounting for 15–20% of breast cancer cases. It lacks estrogen (ER) and progesterone (PR) receptors and shows minimal or absent expression of HER2, making it unresponsive to endocrine or HER2-targeted therapies (Kim, 2025; Sabit et al., 2025). Clinically, TNBC is associated with rapid progression, early metastatic spread, and significantly poorer survival outcomes, with five-year survival rates approximately 8–16% lower than hormone receptor-positive subtypes (Nair et al., 2024; Shrivastava et al., 2022). Although chemotherapy remains the backbone of management in neoadjuvant, adjuvant, and metastatic settings, systemic exposure often induces severe off-target toxicity (Eapen et al., 2025). These challenges reinforce the need for selective, tumor-directed treatment strategies capable of improving efficacy while minimizing collateral damage.

Phytochemicals have emerged as an attractive class of anticancer agents due to their multi-targeted mechanisms and favorable safety profiles. Among them, the isoquinoline alkaloid berberine (BBR) exhibits wide pharmacological activity, including anticancer, antimicrobial, anti-inflammatory, and antioxidant effects (Fan et al., 2025; Liu et al., 2019; Rauf et al., 2021). In breast cancer models, BBR suppresses cell proliferation, induces apoptosis, and inhibits invasion (Kashyap et al., 2022). Mechanistically, BBR can activate TP53 and elevate intracellular reactive oxygen species (ROS), leading to mitochondrial membrane depolarization, altered Bcl-2/BAX expression, and subsequent release of apoptosis-inducing factor and cytochrome c. In TNBC, BBR further attenuates inflammatory signaling by inhibiting NLRP3 inflammasome activation through downregulation of P2X7 and pro-caspase-1 (Redza-Dutordoir & Averill-Bates, 2016). However, its clinical translation is restricted by poor solubility, low permeability, rapid metabolism, and short plasma half-life (Ai et al., 2021; Asghari et al., 2025).

Receptor-mediated targeting is especially relevant for TNBC, where folate receptors (FRs) are overexpressed on tumor cells. Folic acid (FA), a non-immunogenic and thermally stable ligand with high FR affinity, has been extensively used to facilitate selective cellular uptake through folate receptor-mediated endocytosis (Ahmadi et al., 2024; Bellotti et al., 2021). This strategy increases intratumoral drug accumulation while minimizing nonspecific exposure. Nanotechnology-based delivery systems offer a rational solution to overcome these pharmacokinetic limitations and improve therapeutic outcomes. Nanoliposomes are ideally

suited for the encapsulation and delivery of berberine. Their biocompatible phospholipid bilayer provides structural stability, protects encapsulated molecules from premature degradation, and enables controlled release (Majumdar et al., 2024; Rudzińska et al., 2024). When functionalized with FA, nanoliposomes combine passive targeting through enhanced permeability and retention with active receptor-mediated uptake, ensuring preferential localization in FR-overexpressing TNBC cells. This dual targeting approach improves bioavailability, enhances intracellular accumulation, and increases therapeutic index while reducing systemic toxicity.

This study aimed to develop folic acid-functionalized, berberine-loaded nanoliposomes (FA-Lipo) for targeted treatment of triple-negative breast cancer (TNBC), which overexpresses folate receptors. A Quality by Design (QbD) approach with Central Composite Design was used to optimize key formulation parameters for particle size and entrapment efficiency. The optimized FA-Lipo was characterized for size, zeta potential, and morphology, confirming stable surface functionalization. In vitro evaluations showed markedly improved uptake, cytotoxicity, oxidative stress, apoptosis, and genotoxicity for FA-Lipo compared with non-functionalized liposomes and free berberine. These findings demonstrate that folate-targeted nanoliposomes provide selective delivery and superior therapeutic activity against TNBC.

2. Materials and Methods

2.1. Chemicals

Berberine Chloride was procured from Dabur India Pvt Ltd. Phosphatidylcholine (>94%) and Cholesterol were purchased from Central Drug House Pvt. Ltd, New Delhi. Folic acid, Rhodamine, and Cetyl trimethyl ammonium bromide (CTAB) were obtained from Sigma Aldrich. Ethanol and 2, 2- diphenyl-1-picrylhydrazyl (DPPH) were procured from Loba Chemie Pvt. Ltd., India. MDA-MB-231 cell line was brought from National Centre for Cell Science (NCCS) Pune. All drug and buffer solutions were freshly prepared before use. All other reagents used were of analytical grade.

2.2. QbD based Optimization of BBR-loaded Nanoliposomes (BBR–NLs)

Quality Target Product Profile (QTPP): In line with the Quality by Design (QbD) approach for pharmaceutical development, a Quality Target Product Profile (QTPP) was established to guide the formulation of folic acid-functionalized, berberine chloride-loaded nanoliposomes

(BBR–NLs). The primary objective was to enhance the formulation's biopharmaceutical properties and ensure targeted therapeutic efficacy against triple-negative breast cancer (TNBC) (Namjoshi et al., 2020; Pramod et al., 2016). The QTPP outlined key quality attributes that collectively determine the product's clinical performance, such as dosage form, physical characteristics, route of administration, drug strength, and stability requirements. Within this framework, BBR–NLs were conceptualized as a nanoliposomal dispersion optimized for high entrapment efficiency and desirable particle size. This design aimed to improve cytotoxic potential, extend systemic circulation time, and facilitate efficient intracellular delivery, while maintaining physicochemical stability throughout the intended shelf life (Alshaer et al., 2023; Pathak et al., 2024).

Critical Quality Attributes (CQAs): To meet the predefined Quality Target Product Profile (QTPP), a set of Critical Quality Attributes (CQAs) was identified, focusing on physicochemical and formulation parameters directly related to the safety, efficacy, and stability of the BBR–NLs. The selected CQAs included zeta potential, which governs colloidal stability and aggregation behavior; entrapment efficiency (EE%), determining the drug loading capacity; particle size, a key factor for tumor penetration and cellular uptake; polydispersity index (PDI), reflecting the uniformity of liposome size distribution; and formulation pH, ensuring physiological compatibility (Mittal et al., 2023). These attributes were chosen based on their well-established significance in optimizing nanoliposome-based drug delivery systems, as supported by existing scientific literature.

Critical Material Attributes (CMAs) and Critical Process Parameters (CPPs): Both the properties of raw materials (CMAs) and the processing conditions (CPPs) used during formulation play a pivotal role in determining the overall quality of BBR–NLs. Key CMAs include the concentration of berberine chloride, the phosphatidylcholine-to-cholesterol ratio, and the organic-to-aqueous phase ratio, all of which significantly influence vesicle size, stability, and entrapment efficiency (Pramod et al., 2016). Correspondingly, the identified CPPs—such as injection rate, stirring speed, temperature during injection, and solvent evaporation conditions—were recognized as critical determinants of vesicle formation and final product quality. Maintaining these parameters within statistically optimized ranges is essential to ensure batch-to-batch uniformity, reproducibility, and consistent formulation performance.

Risk Assessment: To establish the causal relationships between Critical Material Attributes (CMAs), Critical Process Parameters (CPPs), and their potential influence on the identified

Critical Quality Attributes (CQAs), a systematic risk assessment was performed (Mittal et al., 2022). An Ishikawa (fishbone) diagram was employed to visually represent these relationships, enabling the identification of high-risk factors that could significantly impact key product characteristics. The outcomes of this assessment allowed for the prioritization of critical formulation and process parameters, guiding subsequent experimental optimization and process control efforts.

Design of Experiment (DoE): The formulation was optimized using Design Expert® software version 22.0 (Stat-Ease Inc., Minneapolis, MN, USA) following a Response Surface Methodology (RSM) approach. The objective was to systematically evaluate the influence of key formulation and process variables on the physicochemical properties of the developed system (Ahmed et al., 2018). Based on preliminary experiments and literature evidence, three independent variables were selected: (i) lipid quantity (50–120 mg), (ii) drug amount (5–10 mg), and (iii) water-to-ethanol ratio (3–5). The dependent responses included particle size (Y_1)—targeted for minimization—and entrapment efficiency (Y_2)—targeted for maximization (Table 1).

To minimize confounding effects, specific process parameters were kept constant: the cholesterol-to-lipid ratio was maintained at 1:2, stirring speed at 1000 rpm, and stirring time at 60 minutes. The RSM design generated coded factor levels, including axial (±α) and central points, to develop a quadratic model capable of predicting optimal formulation conditions. This systematic Design of Experiments (DoE) approach provided a comprehensive understanding of the factor–response relationships, enabling robust and reproducible formulation optimization.

Table 1: Design of Experiment Variables

Independent variables	**Levels**				
	+2	+1	0	-1	-2
Factor 1: Amount of Lipid (mg)	26.137	50	85	120	143.86
Factor 2: Amount of Drug (mg)	3.295	5.0	7.5	10.0	11.704
Factor 3: Water: Ethanol	2.318	3	4	5	5.681
Dependent variables	**Constraints**				
Response 1: Size (nm)	Minimum				
Response 2: Entrapment Efficiency	Maximum				

Fixed Variables	Fixed values
Stirring speed	1000 rpm
Stirring time	60 min
Cholesterol: Lipid	1:2

2.3. Preparation of Berberine Chloride-Loaded Nanoliposomes (BBR–NLs)

The solvent injection method was employed to prepare both berberine chloride-loaded nanoliposomes (BBR–NLs) and blank nanoliposomes (NLs). For the preparation of blank NLs, phosphatidylcholine and cholesterol were dissolved in 5 mL of 100% ethanol to form the organic phase, which was maintained at 60 °C. Using a 5 mL syringe fitted with a 24-gauge needle, this organic solution was injected into distilled water preheated to 60 °C, under continuous magnetic stirring at 1000 rpm. The resulting mixture was then subjected to solvent evaporation to facilitate the formation of empty nanoliposomal vesicles (Ben-Fadhel et al., 2022; Kotouček et al., 2020).

Similarly, for the preparation of drug-loaded nanoliposomes, berberine chloride, phosphatidylcholine, and cholesterol were dissolved in 100% ethanol to form the organic phase. This solution was injected into distilled water at 60 °C under the same stirring conditions (1000 rpm), followed by solvent evaporation to yield BBR–NLs. The solvent injection technique was selected due to its simplicity, high entrapment efficiency, and its ability to produce nanoparticles with smaller sizes compared to other preparation methods.

2.4. Preparation of FA-Coated Nanoliposomes (FA-Lipo)

The uncoated nanoliposomes have a negative surface charge, indicating that they are intrinsically anionic due to their phospholipid makeup. Cetyltrimethylammonium bromide (CTAB) was added to the liposomes to make them cationic in order to promote folic acid (FA) surface functionalization through electrostatic interaction. In short, phospholipid, cholesterol, and berberine (BBR) were co-dissolved with 10 mg of CTAB in ethanol (quantities according to the optimal formulation). A pre-emulsion was created by gradually adding the ethanolic lipid–drug phase to the aqueous phase while stirring constantly. After that, ethanol was evaporated at lower pressure to produce cationic nanoliposomes loaded with BBR (Bian et al., 2024; Saberian et al., 2025).

Separately, FA was dissolved in water and stirred for 60 minutes to create aqueous FA solutions at concentrations of 0.01%, 0.05%, 0.1%, and 0.2% (w/v). In order to coat FA over nanoliposomes, 5 mL of FA solution and 10 mL of cationic nanoliposome suspension were combined and gently stirred for 4 hours at room temperature. This allowed the anionic FA to electrostatically adsorb onto the cationic liposomal surface.

2.5. Characterization of nanoliposomes

2.5.1. Particle size and size distribution

The mean particle size and polydispersity index (PDI) of blank nanoliposomes, berberine-loaded nanoliposomes (BBR-Lipo), and folic acid-functionalized nanoliposomes (FA-Lipo) were determined using an Anton Paar Litesizer via dynamic light scattering (DLS), with data acquisition through *Kalliope*™ software. Samples were placed in disposable polystyrene cuvettes and analyzed at 25 ± 2 °C under a fixed backscattering angle of 173°, with each measurement performed in triplicate (n = 3). The DLS technique was selected for its high sensitivity in nanoscale particle characterization, while the 173° backscattering configuration minimized multiple scattering effects, improving accuracy in turbid dispersions. Polystyrene cuvettes, owing to their optical clarity and minimal background interference, ensured reliable light scattering detection, and maintaining a constant temperature reduced viscosity-related variability. Results are expressed as mean ± standard deviation (SD) (Ashhar et al., 2021).

2.5.2. Zeta Potential

Zeta potential, a key indicator of the electrostatic surface charge of colloidal particles, serves as a predictive parameter for formulation stability; values approaching ±30 mV generally signifies sufficient electrostatic repulsion to prevent aggregation. The zeta potential of blank nanoliposomes, berberine-loaded nanoliposomes (BBR-Lipo), and folic acid-functionalized nanoliposomes (FA-Lipo) was measured using an Anton Paar Litesizer 500, with data acquisition and analysis performed via *Kalliope*™ software. Measurements were conducted in disposable folded capillary cells at 25 ± 2 °C, applying phase analysis light scattering (PALS) to determine electrophoretic mobility, which was subsequently converted to zeta potential using the Smoluchowski approximation. All analyses were performed in triplicate (n = 3), and results are expressed as mean ± standard deviation (SD) (Mittal et al., 2021).

2.5.3. Surface Morphology using TEM and SEM

Electron microscopy techniques were employed to evaluate the morphology and confirm the size of the prepared nanoliposomes. For Transmission Electron Microscopy (TEM) analysis, nanoliposome samples (50 µL) were diluted with an equal volume of double-distilled water and carefully applied to a carbon-coated copper grid. Excess sample was removed with filter paper, and the grid was stained with uranyl acetate to enhance contrast. After gentle rinsing with distilled water to remove residual stain, the grids were air-dried before visualization using a Tecnai G2-20 Transmission Electron Microscope (FEI, USA) (Pathak et al., 2024; Ramana et al., 2010).

For Scanning Electron Microscopy (SEM) analysis, samples were coated with a thin conductive layer of gold to enhance electron conductivity and subsequently mounted as a thin film in the sample holder. Negative staining was carried out using a 2% (w/v) phosphotungstic acid solution, followed by incubation at ambient temperature for several hours before imaging. Micrographs were obtained using a Scanning Electron Microscope (EVO 18; ZEISS Group, Germany). (Karpuz et al., 2021).

2.5.4. Entrapment Efficiency and Drug Loading

The percentage entrapment efficiency (%EE) was determined by an indirect method, wherein the free drug present in the supernatant after centrifugation of the liposomal formulation was quantified, and the remaining drug was considered to be entrapped in nanoliposomes. Briefly, 10 mL of the liposomal formulation was centrifuged at 16,000 rpm for 30 minutes using a REMI C-24 Plus CPR-2 Plus centrifuge. The supernatant was collected and analyzed using a UV-Visible Spectrophotometer (UV-1800, Shimadzu, Japan) at 346 nm to determine the unentrapped drug content. The %EE was calculated based on the difference between the total drug and the unentrapped drug. For drug loading (%DL), the pellet obtained after centrifugation was dissolved in ethanol and analyzed by UV spectrophotometry to quantify the amount of drug associated with the nanoparticles relative to their total weight (Alshaer et al., 2023; Mittal et al., 2023).

2.5.5. In-vitro Drug Release Studies

The in-vitro release of berberine from nanoliposomal formulations (BBR-Lipo and FA-Lipo) was evaluated by the dialysis membrane method, a standard procedure to study sustained-release behavior of nanocarriers. Formulations containing an equivalent of 1.6 mg berberine

(BBR) were placed in pre-soaked dialysis bags (molecular weight cut-off 12–14 kDa) and suspended in 250 mL phosphate buffer (pH 7.4) maintained at 37 ± 2 °C with continuous stirring (100 rpm). At predetermined intervals (0.5–72 h), 2 mL aliquots were withdrawn and replaced with equal volumes of fresh buffer to maintain sink conditions. The amount of released BBR was quantified spectrophotometrically at 346 nm. All measurements were performed in triplicate, and data were expressed as mean ± SD (Ansari et al., 2011; Huang et al., 2013).

2.6. Cell Line Studies

Cell Culture

MDA-MB-231 human triple-negative breast cancer (TNBC) cells were obtained and cultured in Dulbecco's Modified Eagle Medium (DMEM) supplemented with 10% fetal bovine serum (FBS) and 1% antibiotic solution (100 U/mL penicillin and 100 µg/mL streptomycin). Cells were maintained at 37 °C in a humidified atmosphere containing 5% CO_2 using a CO_2 incubator (Thermo Fisher Scientific, USA). Subcultures were carried out twice weekly, and cells in the logarithmic growth phase were used for all experiments (Bennett, 2025).

2.6.1. In-vitro Cell Cytotoxicity (MTT) Assay

The cytotoxic potential of free berberine (BBR), berberine-loaded nanoliposomes (BBR-Lipo), and folic-acid-functionalized nanoliposomes (FA-Lipo) was evaluated using the MTT assay. MDA-MB-231 cells were seeded in 96-well plates (5×10^3 cells/well) and allowed to attach overnight. Cells were then treated with varying concentrations of each formulation (25, 50, 100, and 200 µg/mL) and incubated for 24 h under standard conditions. Subsequently, 20 µL of MTT reagent (5 mg/mL in PBS) was added to each well and incubated for 4 h at 37 °C, allowing viable cells to convert MTT to insoluble formazan crystals. The medium was replaced with 100 µL of DMSO to solubilize the crystals, and absorbance was measured at 562 nm using a microplate reader (Synergy HT, BioTek, USA). Cell viability (%) was calculated relative to untreated controls. All assays were performed in triplicate, and results were expressed as mean ± SD (Moloudi et al., 2024).

2.6.2. Reactive Oxygen Species (ROS) Measurement (DCFDA Assay)

Intracellular ROS generation was quantified using the 2′,7′-dichlorofluorescein diacetate (DCFDA) assay. MDA-MB-231 cells were cultured in DMEM with 10% FBS and seeded in 6-

well plates (2×10^5 cells/well). After overnight attachment, cells were treated with BBR, BBR-Lipo, or FA-Lipo at an equivalent BBR concentration of 50 µg/mL for 6 h. Following treatment, cells were washed with PBS and incubated with 25 µM DCFDA in serum-free medium for 45 min at 37 °C in the dark. Cells were then rinsed, and fluorescence intensity was measured using a spectro-fluorimeter (Shimadzu RF-6000) at 485 nm excitation / 529 nm emission. Representative fluorescence micrographs were captured using an inverted fluorescence microscope (20×, green filter) (Čapek & Roušar, 2021; Eruslanov & Kusmartsev, 2010) .

2.6.3. Apoptosis Detection (Annexin V/PI Assay)

Apoptotic cell death was assessed using an Annexin V-FITC/Propidium Iodide (PI) dual-staining assay. MDA-MB-231 cells (5×10^5 cells/well) were seeded in 6-well plates and treated for 24 h with BBR, BBR-Lipo, or FA-Lipo at concentrations equivalent to their IC_{50} values. After treatment, cells were harvested using mild trypsinization, washed twice with cold PBS, and resuspended in 500 µL of 1× binding buffer. To each sample, 5 µL Annexin V-FITC and 5 µL PI (50 µg/mL) were added, followed by 15 min incubation at room temperature in the dark. Fluorescence was analyzed using flow cytometry (BD FACS Calibur, USA) with FL1 (FITC) and FL2 (PI) detection channels (Alshehade et al., 2024; Lakshmanan & Batra, 2013).

2.6.4. Cellular Uptake Studies

Cellular uptake studies were performed in MDA-MB-231 human triple-negative breast cancer cells to evaluate the internalization efficiency of folic acid–functionalized nanoliposomes compared with non-functionalized liposomes. Rhodamine B (RhB) was employed as a fluorescent probe, replacing berberine in equivalent quantity during formulation, while maintaining the same preparation procedure as described for BBR-Lipo. Two formulations were prepared: Rhodamine B-loaded nanoliposomes (R-Lipo) and folic acid-coated Rhodamine B-loaded nanoliposomes (FA-R-Lipo).

MDA-MB-231 cells (1×10^5 cells/well) were seeded in 12-well plates and allowed to adhere for 24 h at 37 °C, 5% CO_2, and 95% relative humidity. After attachment, cells were treated with the respective formulations (diluted to the working concentration in complete DMEM medium) and incubated for 4 h under standard conditions to allow nanoparticle uptake. Following incubation, the cells were washed three times with cold PBS to remove unbound formulations, detached using 0.25% trypsin–EDTA, and centrifuged at 1500 rpm for 5 min (Atabakhshi-

Kashi et al., 2021; Gong et al., 2019). The resulting cell pellets were resuspended in 500 µL PBS, and intracellular fluorescence intensity was quantified by flow cytometry (BD FACSCalibur, USA) using an excitation wavelength of 540 nm and emission detection at 625 nm.

2.6.5. Determination of Oxidative Stress

MDA-MB-231 human breast cancer cells were cultured in DMEM supplemented with 10% FBS and maintained at 37 °C in a humidified 5% CO_2 incubator. Upon reaching approximately 80% confluence, cells were treated with free berberine (BBR), BBR-loaded nanoliposomes (BBR-Lipo), or folic acid-functionalized nanoliposomes (FA-Lipo) at their respective IC_{50} concentrations for 24 h. Following incubation, cells were trypsinized, centrifuged at 1500 rpm for 10 min, and washed twice with chilled PBS. The resulting pellets were lysed in ice-cold buffer (10 mM Tris-HCl, pH 7.4; 250 mM sucrose; 0.2 mM PMSF; 0.2 mM leupeptin; 0.3 mM aprotinin; 0.5 mM EDTA; 0.1 mM pepstatin) and kept on ice for 30 min. Lysates were sonicated and centrifuged at 10,000 rpm for 30 min at 4 °C, and the supernatants were collected for biochemical estimation of oxidative stress markers including Lactate Dehydrogenase (LDH), Nitric Oxide (NO), Superoxide Dismutase (SOD), Reduced Glutathione (GSH), and Glutathione S-transferase (GST). Protein content was normalized for all samples before analysis (Katerji et al., 2019).

2.6.5.1. LDH Assay

LDH activity, an indicator of cell membrane damage, was determined following the method of Kumar et al., 2018 using a commercial LDH Toxicology Assay Kit. Briefly, 100 µL of the cell-free supernatant was mixed with 20 µL of 30 mM sodium pyruvate and 160 µL of 6.6 mM NADH, and the decrease in absorbance at 340 nm was monitored spectrophotometrically, reflecting the rate of NADH oxidation to NAD^+. LDH activity was expressed as nM/mg protein (Freyer & Harms, 2017).

2.6.5.2. Nitric Oxide (NO) Assay

Nitric oxide production was quantified by the Griess reaction, which measures nitrite accumulation in the medium. Equal volumes (100 µL each) of the cell lysate supernatant and freshly prepared Griess reagent (1% sulfanilamide and 0.1% N-(1-naphthyl) ethylenediamine dihydrochloride in 2.5% orthophosphoric acid) were mixed and incubated for 10 min at room

temperature. The resulting chromophore was measured at 540 nm, and NO levels were expressed as µM/mg protein (Gusti et al., 2021).

2.6.5.3. Superoxide Dismutase (SOD) Assay

SOD activity was determined according to Mittal et al., 2023, based on the enzyme's ability to inhibit the reduction of nitroblue tetrazolium (NBT) by phenazine methosulfate–NADH. The reaction mixture consisted of 0.025 M sodium pyrophosphate buffer (pH 8), 180 µM phenazine methosulfate, and 300 µM NBT. To this, 20 µL of cell-free extract and 20 µL of 780 µM NADH were added sequentially to initiate the reaction. Absorbance was measured at 560 nm for 5 min, and SOD activity was expressed as ng/mg protein (Gusti et al., 2021).

2.6.5.4. Reduced Glutathione (GSH) Assay

GSH levels were estimated using the DTNB method described by Mittal et al., 2023. Briefly, 100 µL of cell-free extract was deproteinized with 20 µL of 5% trichloroacetic acid (TCA) and centrifuged at 1200 rpm for 5 min. The supernatant (45 µL) was mixed with 45 µL of 0.2 M PBS (pH 8) and 20 µL of 10 mM DTNB, and absorbance was recorded at 412 nm after 10 min. GSH concentration was expressed as nM/min/mg protein (Gusti et al., 2021).

2.6.5.5. Glutathione S-transferase (GST) Assay

GST activity was measured according to Leekha et al., 2016, based on the conjugation of GSH with 1-chloro-2,4-dinitrobenzene (CDNB). The reaction mixture contained 100 µL CDNB (100 mM), 100 µL GSH (100 mM), and 9.8 mL PBS (pH 6.5). To this, 20 µL of cell-free extract was added, and absorbance was immediately recorded at 340 nm for 5 min. The rate of CDNB–GSH conjugate formation was used to calculate enzyme activity, expressed as nM/min/mg protein (Gusti et al., 2021).

2.7. Genotoxicity Studies

Genotoxicity studies were conducted using the *Oregon-R* strain of *Drosophila melanogaster* to assess the biosafety of BBR-Lipo and FA-Lipo formulations and to evaluate potential DNA damage or cytotoxic effects on non-cancerous biological tissue. *Drosophila* serves as an established in vivo model for preliminary genotoxicity and nanotoxicology screening due to its genetic similarity to humans and conserved cellular signaling mechanisms .

Fly culture and treatment:

Wild-type *Oregon-R* flies were reared on a standard cornmeal-agar-yeast diet composed of Type I agar, sucrose, cornmeal, and yeast, supplemented with propionic acid and methyl paraben (nipagin) to prevent fungal contamination. Flies were maintained at 25 °C, 60% relative humidity, and a 12 h light/dark cycle. For treatment, third-instar larvae were transferred to diet supplemented with BBR-Lipo or FA-Lipo at concentrations of 5, 10, or 25 µg/mL. Control larvae received only the standard diet. Exposure was maintained until the third-instar larval stage was reached. (Siddiqui et al., 2020)

2.7.1. DAPI Staining of Larval Gut

To assess nuclear morphology and DNA integrity, DAPI staining of larval midguts was performed following Kumar & Bauri et al. (2023). Treated and control larvae were dissected in cold PBS, and isolated guts were fixed overnight in 4% paraformaldehyde at 4 °C. Samples were washed thrice with PBS and permeabilized in PBST (PBS + 0.2% Tween-20) for 3 cycles of 20 min each. After final PBS washes, tissues were mounted on glass slides with 10 µL of 5 µM DAPI in 20% glycerol, covered with coverslips, and incubated in the dark for 5 min. Fluorescent images were captured using a fluorescence microscope (Leica Microsystems, Germany), and nuclei were evaluated for chromatin condensation, nuclear fragmentation, or deformation indicative of genotoxicity (Siddiqui et al., 2020).

2.7.2. Trypan Blue Exclusion Assay

To examine membrane integrity and cytotoxicity in larval gut cells, the trypan blue exclusion method was used. Six third-instar larvae from each treatment group were rinsed with PBS and incubated in 0.4% Trypan Blue solution (Sigma-Aldrich, Merck, Germany) for 30 min on a gentle rocker (ROCKYMAX™). Larvae were subsequently washed in 1× PBS for 10 min to remove excess dye. Samples were examined under a stereomicroscope (Motic SMZ171, Spain) to assess blue-stained (non-viable) versus unstained (viable) cells (Carmona et al., 2015; Siddiqui et al., 2020).

3. Result and Discussion

3.1. Optimization of BBR-Lipo Using Quality by Design (QbD)

The QTPP was established through the QbD approach, which involved the systematic consolidation of quality attributes to achieve optimal therapeutic efficacy and patient safety. Table 2 outlines the QTPP for the development of folic acid–functionalized berberine-loaded nanoliposomes intended for the targeted treatment of triple-negative breast cancer. The critical quality attributes (CQAs) identified for the current study were particle size, polydispersity index (PDI), zeta potential, and entrapment efficiency, as these parameters significantly influence the stability, targeting efficiency, cellular uptake, and overall therapeutic potential of nanoliposomes (Mittal et al., 2022, 2023). Table 3 presents a summary of the CQAs along with their justifications. The selection of these CQAs was based on extensive literature review, prior experimental knowledge, and formulation expertise pertaining to nanoliposome systems. In line with the preliminary risk assessment strategy, a cause-and-effect (Ishikawa) fishbone diagram was constructed to identify and categorize potential formulation and process variables that may impact the CQAs (Pathak et al., 2024). Figure 2 illustrates the fishbone diagram, highlighting various critical material attributes (CMAs) and critical process parameters (CPPs) that could exert a significant influence on the CQAs of the developed nanoliposomes. Following the risk assessment, high-risk parameters were shortlisted from a pool of multiple variables. The results indicated that lipid concentraion, drug concentration, and water: methnol ratio were among the most critical factors impacting the CQAs.

Table 2: Quality Target Product Profile (QTPP) for Nanoliposome Formulation

QTPP Element	**Target**	**Rationale**
Dosage form	Nanoliposome dispersion (colloidal suspension)	Enables encapsulation of hydrophobic berberine chloride and ensures stability in aqueous medium.
Route of administration	*In vitro* studies for potential parenteral or targeted cancer therapy	Parenteral administration preferred for targeted delivery and bypass of first-pass metabolism.
Appearance	Homogeneous, yellowish colloidal dispersion	Uniform vesicle distribution indicates consistent formulation quality; yellow tint due to berberine content.
Sterility	Sterile product	Essential for parenteral use and cell-line studies.

Stability	At least 6 months at 4 °C without significant changes in particle size or EE%	Maintains product quality during storage and experimental timelines.

Table 3: Key Critical Quality Attributes Influencing Nanoliposome Performance

CQA	**Target**	**Rationale**
Particle size	80–200 nm	Ensures enhanced tumor permeability via EPR effect and prevents rapid clearance by the reticuloendothelial system.
Polydispersity index (PDI)	≤ 0.3	Indicates narrow size distribution for predictable pharmacokinetics and stability.
Drug loading	≥ 5% w/w	Sufficient therapeutic payload for effective cytotoxic activity against TNBC cells.
Entrapment efficiency	≥ 70%	Ensures high drug retention within vesicles, reducing dosing frequency.
Zeta potential	±20 to ±40 mV	Provides adequate electrostatic repulsion for colloidal stability during storage.
pH	6.5–7.4	Physiologically compatible for potential intravenous administration.

Design of Experiment (DoE): The formulation was optimized using a Quality by Design (QbD) framework and a Central Composite Design (CCD) under the Design of Experiments (DoE) approach. CCD is a response surface methodology that combines factorial points, axial points, and central points to efficiently model curvature and interaction effects between formulation variables, reducing the total number of experiments required. In this study, the independent variables—lipid concentration, water–ethanol ratio, and drug load—were evaluated against the critical quality attributes (CQAs): particle size and entrapment efficiency. Based on the defined variable ranges, the CCD design recommended 20 experimental runs, including five central points, to ensure model accuracy and reproducibility. The prepared formulations were subsequently characterized as summarized in Table 3.

438 **Table 3:** Response Analysis Data for Optimization of nanoliposomes

	Independent Variables			Dependent Responses	
Formulation code	Amount of Phospholipid (mg)	Amount of drug (mg)	Water: Ethanol ratio	Size(nm)	Entrapment efficiency (%)
F1	50	10	5	168	23
F2	85	7.5	2.318	166.3	25
F3	50	5	5	110	23.2
F4	143.86	7.5	4	268	49
F5	85	7.5	4	56.7	48
F6	85	7.5	5.681	83.2	43
F7	85	7.5	4	70.48	47.5
F8	120	10	5	167.99	34
F9	120	5	3	168.31	33
F10	85	3.295	4	109	39
F11	26.137	7.5	4	124	24
F12	85	7.5	4	74.2	47.8
F13	50	5	3	129	29
F14	85	7.5	4	68.2	48.1
F15	120	5	5	218.3	38
F16	120	10	3	208	47
F17	85	7.5	4	69.4	45
F18	50	10	3	140	32
F19	85	7.5	4	79.3	46.3

F20	85	11.704	4	244.1	47

3.2.1. Response Analysis for Optimization

(i) Impact on particle size:

Particle size is a critical quality attribute influencing the targeting efficiency and therapeutic performance of nanoliposomes. ANOVA analysis of the experimental data revealed that the quadratic model adequately fit the particle size response, with a predicted R^2 of 0.8729 closely aligning with the adjusted R^2 of 0.8563, indicating strong model predictability. The model's signal-to-noise ratio was 45.849, confirming an adequate signal. Statistical evaluation showed that the model terms were significant, with p-values < 0.05. The particle size response was described by the following coded quadratic equation

$$\text{Particle size} = +69.97 + 33.52 \times A + 20.91 \times B - 8.85 \times C - 9.95\ A \times B + 0.1225\ A \times C - 5.38\ B \times C + 42.98 \times A^2 + 36.11 \times B^2 + 17.80 \times C^2$$

Positive coefficients for A and B indicate a direct linear relationship between particle size and the amounts of drug and lipid; increasing either result in larger nanoliposomes. Conversely, the negative coefficient for V suggests an inverse relationship, with higher water:ethanol ratios leading to smaller particle sizes. Interaction and quadratic terms further refine this relationship. Figure 2A illustrates the effects of these independent variables on particle size.

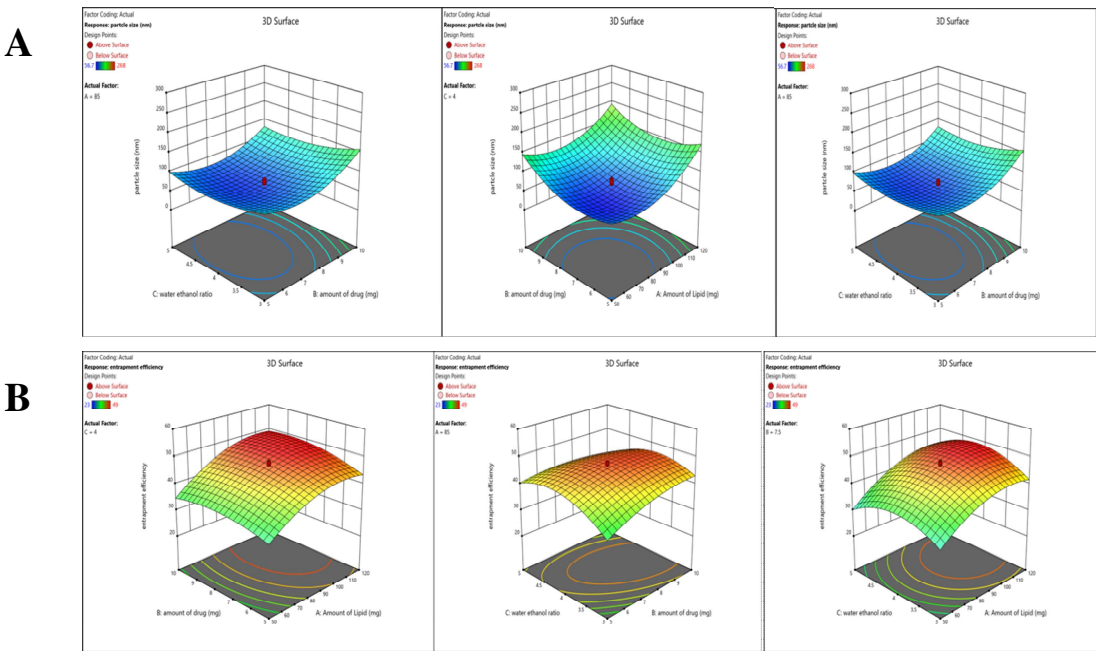


Fig. 2. 3-D plots for the impact of independent variables on A) particle size and B) **Entrapment Efficiency** of BBR-Lipo

(ii) Impact on Percent Entrapment Efficiency:

Fig. 2B illustrates the influence of various factors on entrapment efficiency. Percent entrapment efficiency directly influences the dose of formulation required for the therapeutic action and therefore a prime factor to be optimized in most of the nanformulatuions. It is noticed that mostly it varies between 51.42% and 79.0% in different classes of nanoliposomes. Upon statistical analysis (ANOVA) of experimental data obtained for 20 formulations, a higher R^2 value (0.8056) for the quadratic model was obtained. Also, from the following model-generated equation, the impact of various independent variables on the percent drug entrapment can be analysed.

Entrapment Efficiency= +47.31 +6.36 × A +1.92 ×B +0.5471 ×C + 0.9000 ×A × B +0.8500 ×A×C -2.65 × B×C -4.79× A^2 – 2.49 × B^2- 5.68 ×C^2

The percent drug entrapment for all 20 formulations varied between 23.0% and 49%. The positive coefficient values of independent variables indicate the direct relation between drug entrapment and the amount of drug, lipids, and water to methanol ratio. From the highest coefficient value of A, it's evident that the amount of lipid has the most significant impact on entrapment efficiency, followed by the drug quantity and the water: ethanol ratio. An increase in lipid concentration results in the formation of larger nanoliposomes, thereby enhancing entrapment efficiency. Similarly, as drug concentration rises, more of the drug is encapsulated within the nanoliposomes.

However, increasing the water: ethanol ratio produces smaller nanoliposomes, leading to reduced entrapment efficiency.

3.2. Preparation of nanoliposomes

For developing the most effective formulation, parameters were optimized using the Quality by Design (QbD) approach. The optimized formulation, as predicted by the model, comprised a drug amount of 7.36 mg, a water-to-organic phase ratio of 4:1, and a lipid content of 88.5 mg. Nanoliposomes were subsequently prepared by the solvent injection method, following the principles described by Lasic and colleagues (Lasic, 1988). According to the Bilayer Planar

Fragmentation (BPF) theory, lipids dissolved in ethanol migrate to the interface between the aqueous and organic phases. This interfacial arrangement leads to the formation of planar bilayer fragments. As the organic solvent disperses completely into the aqueous phase, these fragments spontaneously self-assemble into vesicles, resulting in the formation of nanoliposomes.

3.3. Preparation of FA-Lipo

For targeted delivery, the optimized BBR-loaded nanoliposomes were successfully surface-functionalized with folic acid (FA), exploiting the electrostatic interaction between the positively charged CTAB-modified surface and negatively charged carboxyl groups of FA. FA solutions of varying concentrations (0.01%, 0.05%, 0.1%, and 0.2%) were tested to identify the optimal coating ratio. At 0.01% FA, no appreciable change in zeta potential or size was observed, suggesting incomplete coating. At concentrations above 0.1%, aggregation and turbidity were evident, indicating charge overcompensation and colloidal instability. The 0.1% FA concentration provided an optimal balance, yielding uniformly coated nanoliposomes with minimal size variation and stable surface charge reversal, confirming successful conjugation.

The results confirm that electrostatic assembly between CTAB-modified cationic liposomes and anionic folic acid efficiently produced a stable FA-Lipo formulation at 0.1% FA concentration. The shift in zeta potential and the slight increase in particle size serve as direct indicators of successful FA conjugation. Excess FA concentrations likely promoted partial neutralization and interparticle bridging, leading to aggregation, while insufficient FA failed to achieve full surface coverage. Thus, optimizing FA concentration was critical to ensure stable functionalization without compromising liposomal integrity. These findings are consistent with previous studies reporting zeta-potential–guided optimization of FA conjugation for receptor-targeted nanocarriers (Hood et al., 2013; Kumar et al., 2019) .

3.4. Characterization of Blank-Lipo, BBR-Lipo and FA-Lipo

3.4.1. Particle Size and Size Distribution

The particle size of Blank-Lipo was measured at 56.7 ± 2 nm with a PDI of 0.26 (Fig. 5a), indicating a uniform nanoscale dispersion. Upon encapsulation of BBR, the particle size significantly increased to 95.63 ± 2.2 nm with a PDI of 0.23 (BBR-Lipo) (Fig. 5b), suggesting successful drug loading and a modest increase in size likely attributable to the incorporation of

the drug within the bilayer or aqueous core. Further functionalization with FA resulted in a marked size increase to 168.31 ± 2.1 nm with a PDI of 0.26 (FA-Lipo) (Fig. 5c), which can be ascribed to the surface modification and conjugation of FA molecules (Ashhar et al., 2021).

3.4.2. Zeta Potential

The zeta potential of BBR-Lipo was −21.0 ± 0.9 mV (Fig. 5d), reflecting the inherent surface characteristics of the lipid bilayer, which remained unaffected by BBR encapsulation due to the drug's localization within the vesicle. Post-CTAB modification, the surface charge shifted to a highly positive value of 51.9 ± 1.3 mV (Fig. 5e), confirming the cationic nature of the surfactant and its adsorption onto the liposomal surface. Following FA coating, the zeta potential shifted again to −0.6 ± 2.2 mV (Fig. 5f), likely due to the presence of carboxyl groups from FA, which neutralized the positive charge imparted by CTAB. These sequential modifications not only demonstrate the successful stepwise functionalization of liposomes but also highlight the tunability of their physicochemical properties for targeted drug delivery applications. (Geethakumari et al., 2022; Mittal et al., 2021; Parvathaneni et al., 2023).

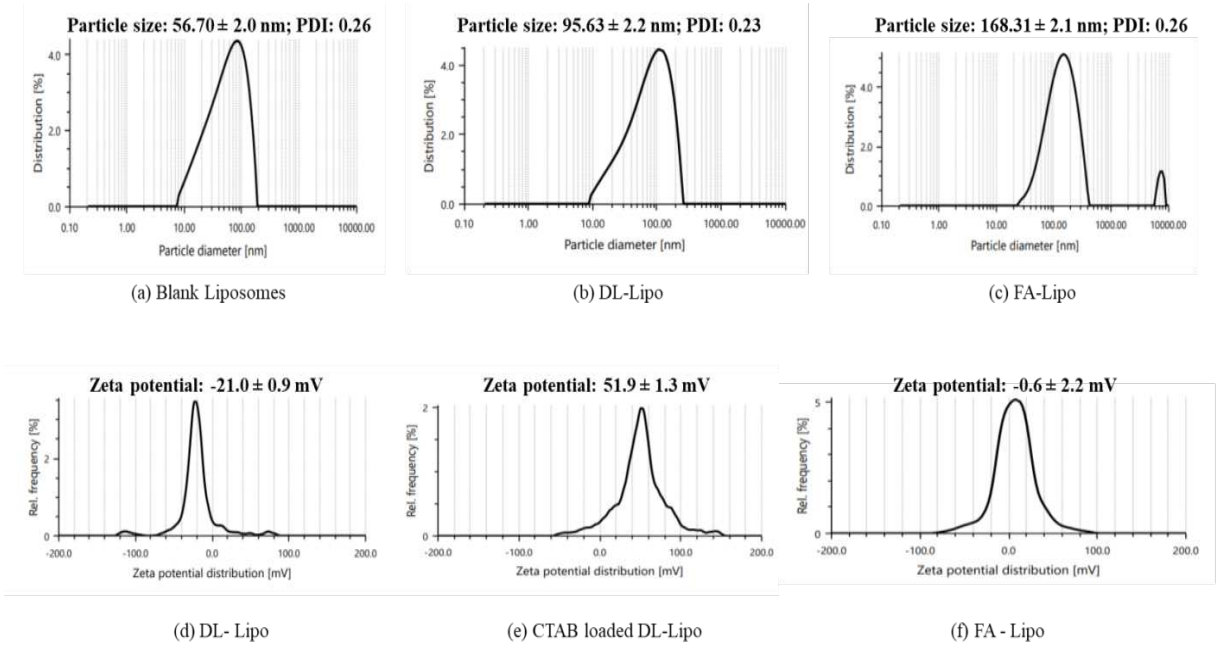


Fig. 5. Particle size distribution and Hydrodynamic diameter of (a) Blank Lipo (b) BBR Lipo and (c) FA Lipo and Zeta potential of (d) BBR-Lipo (e) CTAB treated BBR-Lipo (f) FA Lipo

3.4.3. Surface morphology using TEM and SEM

The TEM images of blank liposomes, BBR-Lipo, and FA-Lipo (Fig. 6a–c) reveal essential structural characteristics at the nanoscale, offering critical insights into their morphology and vesicle integrity. The blank nanoliposomes appear as hollow, spherical entities enclosed by a thin lipid bilayer, indicating the successful formation of vesicular structures essential for encapsulation (Fig 6a). In contrast, the BBR-Lipo exhibited a thicker lipid bilayer compared to the blank nanoliposomes, which suggests the incorporation of the drug both within the aqueous core and the lipid bilayer. This bilayer thickening can be attributed to the intercalation of drug molecules within the lipophilic regions of the nanoliposomes, thereby confirming efficient drug loading (Fig 6b). The FA-Lipo image shows a visibly uneven surface, which serves as a clear indication of FA acid coating on the nanoliposomes (Fig 6c**).** The irregularity in surface texture is likely due to the covalent binding or electrostatic interaction of folic acid molecules with the liposomal surface, signifying successful surface modification aimed at enhancing targeted drug delivery (Siddiqui et al., 2020).

SEM images of blank nanoliposomes, BBR-Lipo, and FA-Lipo (Fig. 6d–f) further corroborate the structural features observed in the TEM analysis, providing complementary morphological evidence. The blank nanoliposomes are visualized as smaller, smooth, and relatively uniform structures, confirming their efficient formulation without any significant aggregation. The smaller size and uniformity of blank nanoliposomes suggest better suspension stability, a desirable trait for drug carriers (Fig 6d**).** The BBR-Lipo images show larger and slightly irregular structures, which align with the presence of the encapsulated drug. The increase in size compared to blank nanoliposomes can be attributed to the additional volume of the drug-loaded within the lipid bilayer and core (Fig 6e). The FA-Lipo, in comparison, appears as a larger structure with an uneven and rough surface. Therefore, this surface irregularity confirms successful folic acid coating (Fig 6f) (Rhee et al., 2010).

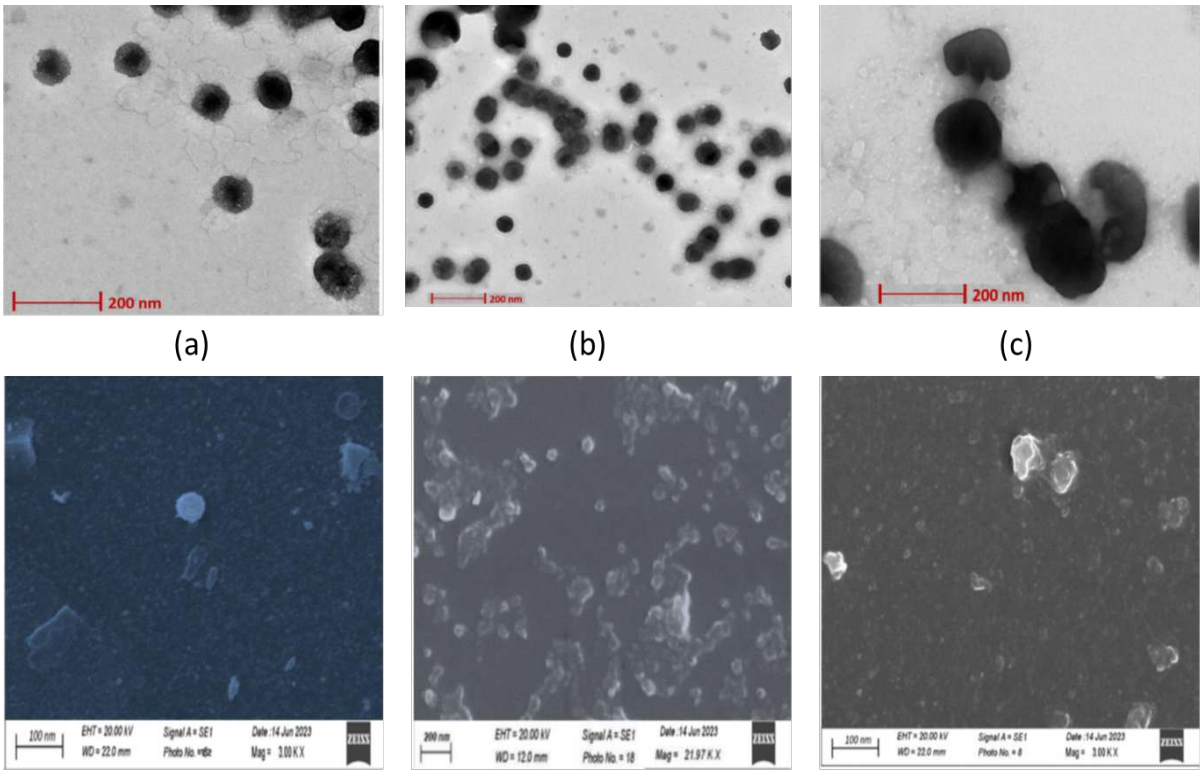


Fig. 6. TEM images of (a) Blank Lipo, (b) BBR-Lipo, and (c) FA-Lipo and SEM Images (d) Blank Lipo, (e) BBR Lipo, and (f) FA Lipo

3.5. Entrapment Efficiency and Drug Loading

The optimized berberine-loaded nanoliposomes (BBR-Lipo) exhibited an entrapment efficiency (%EE) of 47.5 ± 2% and a drug loading (%DL) of 16.05 ± 2%. Following surface functionalization with folic acid, the FA-coated nanoliposomes (FA-Lipo) displayed a moderate decrease in both parameters, with %EE and %DL values of 41.8 ± 2% and 10.75 ± 1.5%, respectively. This slight reduction is attributable to the FA conjugation step, during which folic-acid molecules interact with the outer lipid surface, introducing steric constraints and mild perturbations in bilayer packing that may cause limited drug diffusion or partial leakage during coating (Singh et al., 2016).

The minor decline in entrapment and loading efficiency indicates that the FA-coating process influences liposomal architecture without compromising overall drug retention. Such changes are typical when surface ligands are introduced, as they can alter lipid ordering and interfacial

charge density. Importantly, the maintained encapsulation efficiency (>40%) ensures sufficient payload for therapeutic application while enabling folate-receptor–mediated targeting. These findings are consistent with earlier reports showing that ligand decoration slightly reduces drug content but significantly enhances selective cellular uptake and anticancer efficacy, thereby improving the formulation's overall pharmacological performance (Parvathaneni et al., 2023).

3.6. In-vitro Drug Release Studies

The cumulative release profiles of BBR-Lipo and FA-Lipo are presented in Fig. 7. Both formulations exhibited controlled and sustained release of berberine over 72 h, with no initial burst phase, confirming strong drug–bilayer association and structural integrity of the vesicles. BBR-Lipo released 63 ± 2% of its payload within 72 h, whereas FA-Lipo showed a higher cumulative release of 78 ± 2%, indicating slightly faster diffusion following surface modification. The absence of burst release suggests uniform drug encapsulation within the lipid matrix, minimizing premature leakage and ensuring prolonged availability. The moderately enhanced release from FA-Lipo can be attributed to the presence of folic acid on the surface, which may increase hydrophilicity and slightly loosen lipid packing, thereby facilitating diffusion of the entrapped BBR molecules through the membrane (Kumar et al., 2019).

The release kinetics fitted best to the Higuchi diffusion model ($R^2 > 0.98$), indicating a predominantly diffusion-controlled mechanism governed by the lipid bilayer matrix. The slower release of BBR-Lipo corresponds to a tighter bilayer packing, whereas FA-functionalization introduced mild structural re-organization that accelerated diffusion without causing instability. The sustained and near-linear release profile supports the potential of these nanoliposomes to maintain therapeutic berberine levels for extended periods, reducing dosing frequency and systemic fluctuations. Moreover, the controlled release complements the folate-receptor–mediated uptake mechanism, ensuring steady intracellular availability after targeted delivery. These findings corroborate earlier reports that folate decoration can modulate liposomal membrane permeability while preserving encapsulation efficiency, thereby enhancing pharmacokinetic performance and anticancer efficacy (Jain & Jain, 2016; Patel et al., 2024; Rostami et al., 2023).

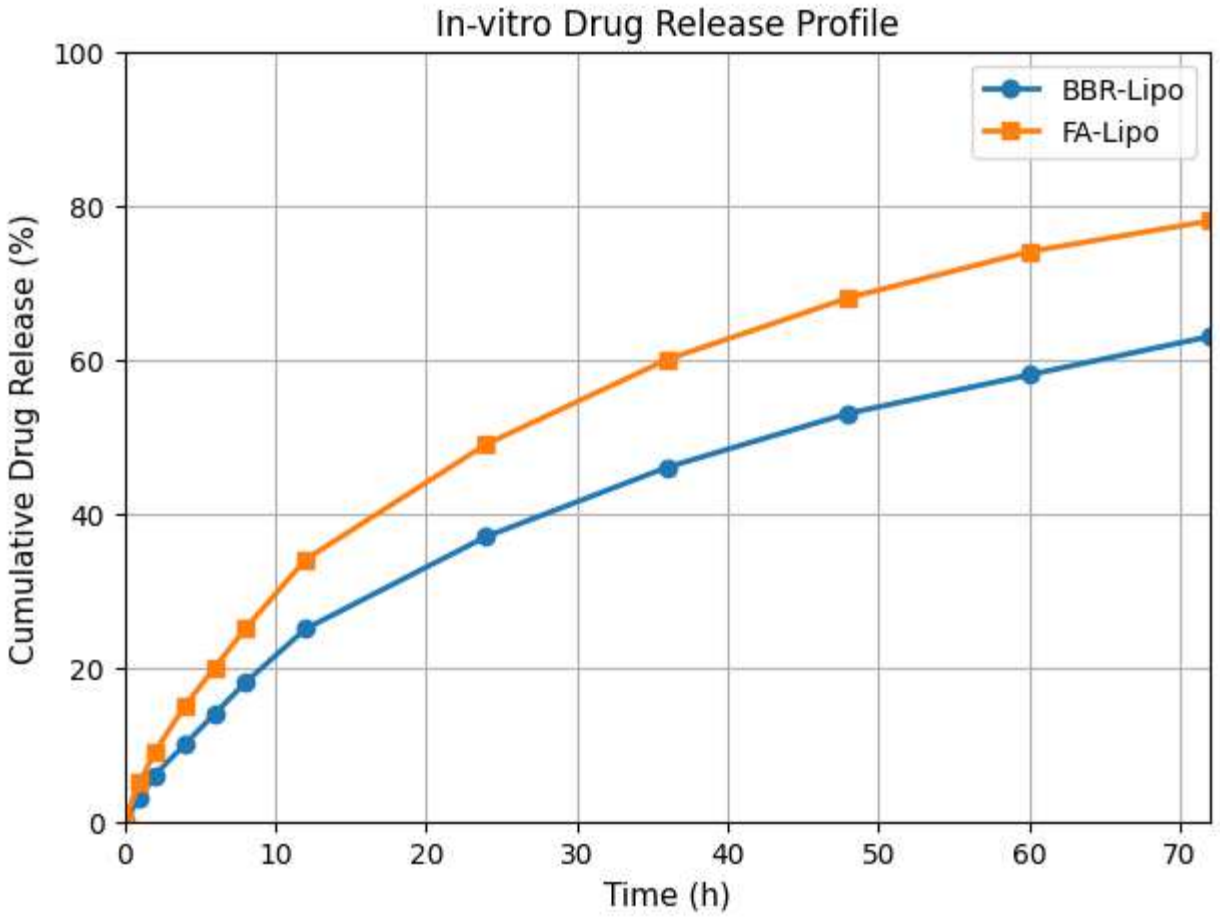


Fig. 7. In-vitro cumulative drug release profile of BBR-Lipo and FA-Lipo over 72 h showing sustained diffusion-controlled release behavior. Values represent mean ± SD (n = 3).

3.7. Cell line studies

3.7.1 In-vitro Cell Cytotoxicity (MTT) Assay

Cytotoxicity was compared across free berberine (BBR), blank liposomes (Blank-Lipo), berberine-loaded liposomes (BBR-Lipo), and folic-acid-functionalized berberine-loaded liposomes (FA-Lipo) (Fig. 8a). Blank-Lipo showed negligible cytotoxicity, confirming vehicle biocompatibility. Free BBR produced a dose-dependent effect (10.45 ± 1.41% to 68.62 ± 1.76% cell death) with an IC_{50} of 120.41 ± 5.32 µM, consistent with apoptosis/oxidative-stress-linked activity yet limited by poor solubility and efflux liability. BBR-Lipo markedly enhanced potency (34.16 ± 9.79% to 78.62 ± 1.48% cell death; IC_{50} 47.65 ± 2.14 µM), attributable to improved apparent solubility, endocytic uptake, and partial circumvention of P-gp–mediated efflux. As expected for FR^+ conditions, FA-Lipo was most potent, achieving 88.77 ± 1.26%

cell death at 200 µM with the lowest IC_{50} (24.72 ± 1.87 µM). This corresponds to a ~4.9-fold increase in potency versus Free BBR (120.41/24.72) and a ~2.0-fold increase versus BBR-Lipo (47.65/24.72), validating folate-receptor-mediated uptake as the dominant driver of enhanced cytotoxicity under our assay conditions. Overall, the potency rank was FA-Lipo > BBR-Lipo > Free BBR ≫ Blank-Lipo, in line with the hypothesized contribution of receptor-targeted endocytosis atop the baseline gains from liposomal encapsulation.

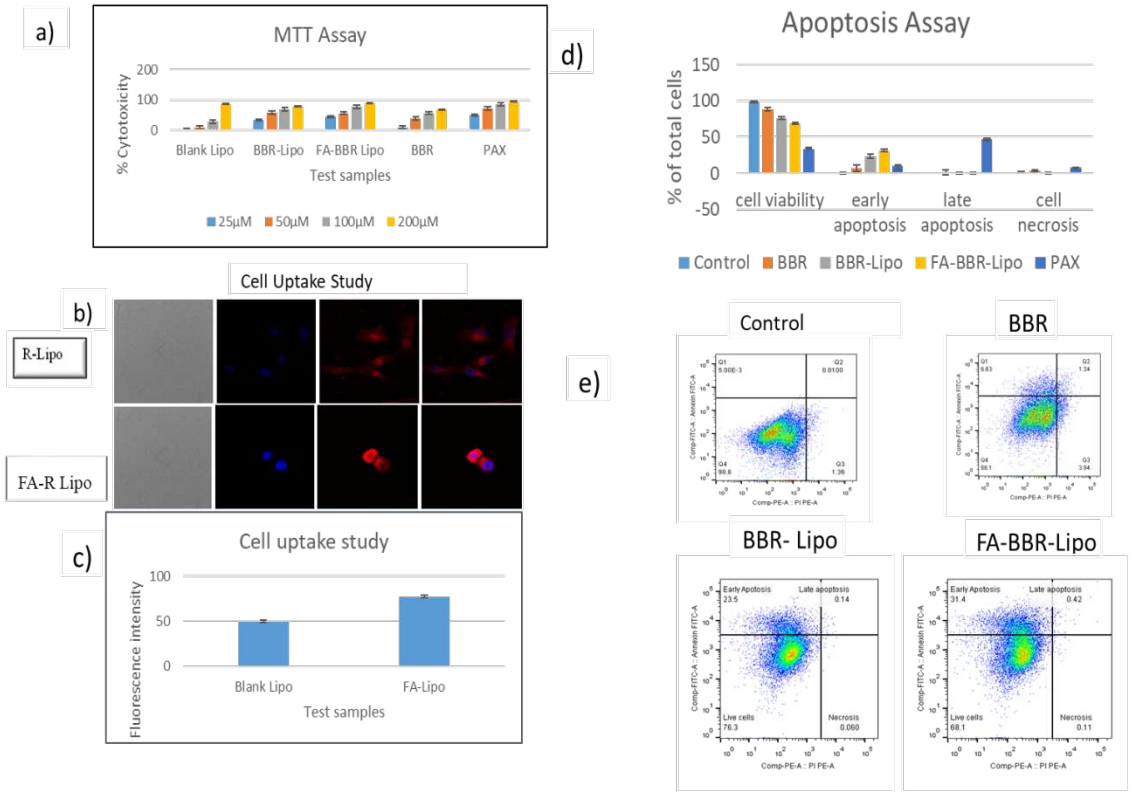


Fig. 8. a) Graphical representation of cytotoxicity of different formulations on MDA-MB-231 cells, b) Qualitative estimation of cellular uptake, c) quantitative estimation of cellular uptake of FA-R-Lipo in MDA-MB-231 cells, d) Graph representing cell viability, early and late apoptosis and necrosis in MDA-MB-231 cells e) Analysis of Annexin V-FITC/PI staining in MDA-MB-231 cells by flow cytometry

The comparative cytotoxicity profile among the four groups—free berberine (BBR), blank liposomes (Blank-Lipo), berberine-loaded liposomes (BBR-Lipo), and folic acid-functionalized berberine-loaded liposomes (FA-Lipo)—revealed a clear enhancement of anticancer activity following liposomal encapsulation and folate receptor (FR)-targeted delivery. Blank-Lipo exhibited minimal cytotoxicity, confirming the inherent biocompatibility of the phospholipid matrix and validating that the observed effects were exclusively due to

berberine. Free BBR demonstrated moderate, dose-dependent cytotoxicity, consistent with its known ability to induce apoptosis through mitochondrial depolarization and reactive oxygen species (ROS) generation (Ibrahim et al., 2023; Kumar et al., 2019). However, its therapeutic efficacy was limited by poor aqueous solubility, rapid efflux via P-glycoprotein transporters, and insufficient intracellular accumulation. Incorporation of BBR into liposomes substantially enhanced its cytotoxic potential, likely due to improved solubilization and facilitated cellular internalization through nonspecific endocytic pathways, resulting in higher intracellular retention of the drug. The FA-Lipo formulation exhibited the most pronounced cytotoxic response, achieving almost complete cell death at higher concentrations and the lowest IC_{50} value among all groups. This enhancement can be attributed to the overexpression of folate receptors on MDA-MB-231 cells, which mediate receptor-specific endocytosis of folate-conjugated nanocarriers, leading to efficient intracellular delivery and amplified pharmacodynamic action. Moreover, the FA-Lipo system likely provided sustained intracellular release of berberine, prolonging its interaction with mitochondrial and nuclear targets responsible for oxidative stress induction and genotoxicity. These findings corroborate previous reports where folate-functionalized liposomal systems achieved superior tumor selectivity and reduced off-target cytotoxicity compared to non-targeted counterparts (Ahmadi et al., 2024; Ye et al., 2014).

3.7.2. Reactive Oxygen Species (ROS) Measurement (DCFDA Assay)

The intracellular ROS levels in MDA-MB-231 cells were quantified using the DCFDA assay, wherein non-fluorescent DCFDA is converted to fluorescent DCF upon oxidation by reactive oxygen species, serving as an indicator of oxidative stress. As shown in Fig. 9, the untreated control group exhibited minimal fluorescence (8.5 ± 1.2 au; Fig. 9a), confirming basal ROS levels under normal physiological conditions. Free BBR induced a moderate increase in ROS (28.9 ± 2.1 au; Fig. 9b), consistent with previous findings that berberine enhances oxidative stress by impairing mitochondrial electron transport and promoting superoxide generation (Hou et al., 2017; Xiong et al., 2022). Incorporation of BBR into liposomes markedly amplified intracellular ROS (57.8 ± 3.4 au; Fig. 9c), which can be attributed to improved solubility, cellular uptake via endocytosis, and sustained intracellular retention of the encapsulated drug. Notably, FA-Lipo exhibited the highest ROS signal (86.4 ± 2.7 au; Fig. 9d)—nearly threefold higher than free BBR and comparable to the paclitaxel-treated positive control (Fig. 9e). The enhanced oxidative response arises from folate receptor-mediated endocytosis, which promotes

selective intracellular delivery of berberine in FR-overexpressing TNBC cells. The increased intracellular availability facilitates mitochondrial localization of berberine, where it accelerates ROS generation. The resultant ROS surge acts as an upstream driver of mitochondrial membrane depolarization, oxidative DNA damage, and activation of apoptotic pathways. These findings are consistent with previous reports showing that folate-functionalized nanocarriers amplify oxidative and genotoxic stress in tumor cells by receptor-guided uptake and improved drug bioavailability (Hu et al., 2023; Zhang et al., 2022). Collectively, the data confirm the rank order of oxidative stress induction as FA-Lipo > BBR-Lipo > Free BBR ≫ Blank/Control, highlighting the critical contribution of FR-targeted liposomal design in maximizing berberine-mediated redox cytotoxicity in triple-negative breast cancer cells.

The DCFDA assay results clearly demonstrate that FA-Lipo induces the highest intracellular ROS generation among all tested formulations, confirming that folate receptor (FR)–targeted delivery significantly amplifies berberine's redox activity in MDA-MB-231 cells. The enhanced oxidative stress observed with FA-Lipo is a direct consequence of receptor-mediated endocytosis, which facilitates efficient internalization and mitochondrial localization of berberine, a known modulator of mitochondrial respiratory complexes (Marshalek et al., 2016; Siddiqui et al., 2020). The elevated ROS levels initiate oxidative damage to cellular macromolecules, leading to lipid peroxidation, mitochondrial depolarization, and activation of intrinsic apoptotic signaling. This effect is further magnified by the sustained intracellular retention of liposomal berberine, ensuring prolonged oxidative burden compared to the transient exposure seen with free drug. The moderate ROS induction by BBR-Lipo suggests that liposomal encapsulation alone improves cellular uptake and intracellular release, yet the absence of receptor targeting limits its intracellular concentration relative to FA-Lipo. In contrast, free BBR exhibited only modest ROS elevation, consistent with its poor solubility and efflux-mediated clearance, whereas Blank-Lipo maintained basal ROS levels, verifying liposomal biocompatibility (Schieber & Chandel, 2014; Su et al., 2019). The positive correlation between ROS generation and cytotoxic potency (IC_{50}: FA-Lipo < BBR-Lipo < BBR) strongly supports oxidative stress as a principal mechanism underlying berberine-induced apoptosis in triple-negative breast cancer. These findings align with previous reports that nanocarrier-mediated and receptor-targeted delivery of redox-active phytochemicals can overcome pharmacokinetic barriers, enhance mitochondrial accumulation, and trigger ROS-dependent DNA damage responses, culminating in irreversible cell death (Li et al., 2016; Zhang et al., 2022). Overall, the data reinforce that QbD-engineered, folate-decorated liposomal

systems effectively exploit oxidative stress pathways to intensify genotoxic and apoptotic effects in FR-overexpressing TNBC cells, thereby offering a mechanistically superior approach to targeted chemotherapy.

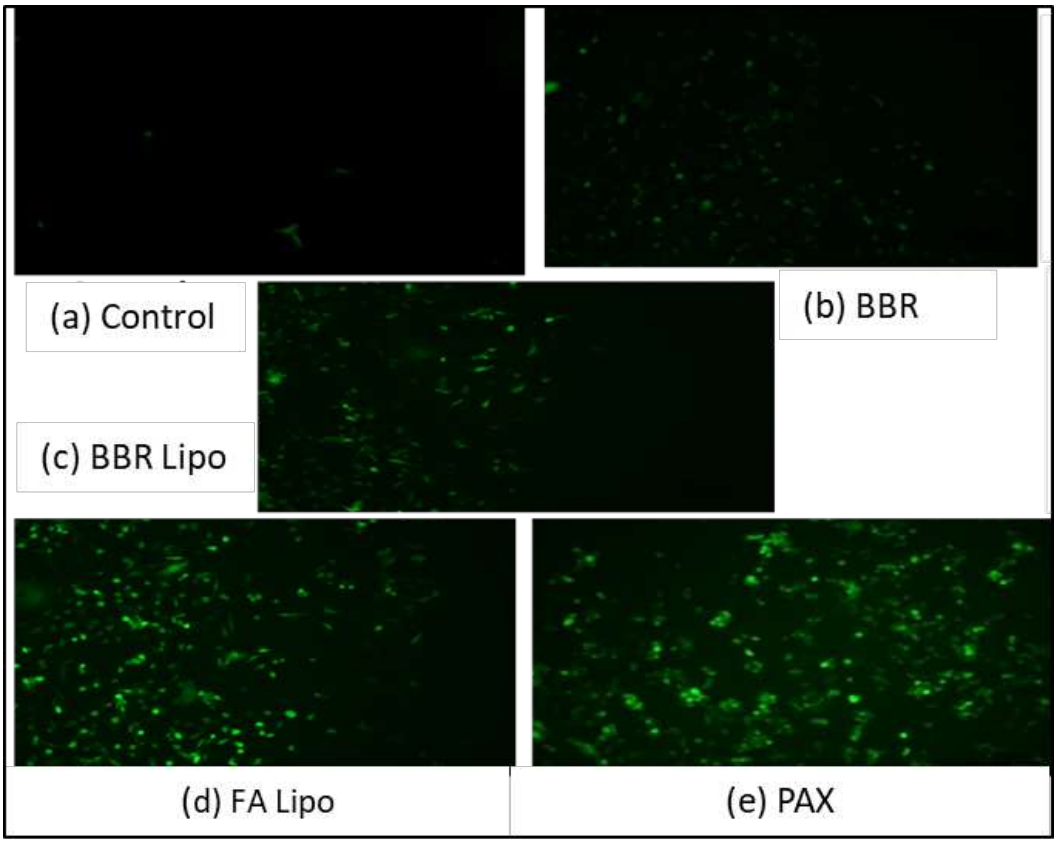


Fig. 9. Total ROS levels assessed by DCFDA Assay: Fluorescence Intensity in MDA-MB 231 Cell lines of (a) Control (b) BBR (c) BBR-Lipo (d) FA-Lipo and (e) PAX.

3.7.3. Apoptosis Detection (Annexin V/PI Assay)

Apoptosis induction by the nanoliposomes was evaluated using an Annexin V–based flow-cytometric assay that detects phosphatidylserine (PS) externalization, a hallmark of early apoptosis. MDA-MB-231 cells were treated with IC_{50} concentrations of free berberine (BBR), BBR-loaded liposomes (BBR-Lipo), and folic-acid-functionalized BBR-loaded liposomes (FA-Lipo). Cells exposed to free BBR showed primarily viable populations (87.9 ± 1.0%) with limited early (7.2 ± 0.3%) and late apoptosis (2.4 ± 0.2%), indicating modest intrinsic cytotoxicity. BBR-Lipo treatment markedly enhanced apoptosis, reducing viable cells to 74.6 ± 0.8% and increasing early apoptotic cells to 21.8 ± 0.5%, while late apoptosis and necrosis remained minimal (2.9 ± 0.3% and 0.7 ± 0.1%, respectively). FA-Lipo demonstrated the

strongest pro-apoptotic effect, reducing cell viability to 34.1 ± 0.6% and elevating early and late apoptotic fractions to 38.6 ± 0.4% and 26.8 ± 0.3%, respectively, with negligible necrosis (0.5 ± 0.1%) [Fig. 8(d–e)].

The order of apoptotic potency followed FA-Lipo > BBR-Lipo > Free BBR ≫ Blank-Lipo, corroborating the cytotoxicity and ROS trends. FA-Lipo triggered the highest apoptosis due to folate-receptor-mediated endocytosis, which enables selective accumulation of berberine within tumor cells, leading to elevated mitochondrial oxidative stress and caspase activation. BBR-Lipo also enhanced apoptosis through improved intracellular delivery, while free BBR remained less effective because of poor solubility and efflux-mediated elimination (Sun et al., 2018; Zhu et al., 2022).

3.7.4. Cellular Uptake Studies

Cellular uptake of nanoliposomes was examined using Rhodamine B-loaded formulations in MDA-MB-231 cells to evaluate the influence of folic-acid surface functionalization on internalization efficiency. The mean fluorescence intensity (MFI) of cells treated with Rhodamine B-loaded liposomes (R-Lipo) was 48.9 ± 2.3 au [Fig. 8(b)], whereas folate-conjugated Rhodamine B-loaded liposomes (FA-R-Lipo) exhibited a significantly higher MFI of 78.4 ± 2.1 au [Fig. 8(c)]. The ~1.6-fold increase in fluorescence intensity indicates enhanced cellular uptake mediated by folate-receptor interaction.

The uptake hierarchy—FA-R-Lipo > R-Lipo ≫ Blank—confirms that folate conjugation markedly augments liposomal internalization through receptor-mediated endocytosis in FR-positive TNBC cells. The higher intracellular fluorescence of FA-R-Lipo validates successful surface functionalization and supports the mechanistic basis for its superior cytotoxic and pro-apoptotic performance. These observations agree with reports by Nguyen-Huu and associates , which demonstrated that FA-decorated liposomes show preferential accumulation in folate-receptor-overexpressing cells (Nguyen-Huu et al., 2024). Overall, the findings establish that folate-targeted nanoliposomes achieve higher intracellular drug exposure and therapeutic efficiency through specific receptor-ligand interactions and improved endocytic trafficking.

3.7.5.1. LDH Assay

The lactate dehydrogenase (LDH) assay was employed to assess cell membrane integrity disruption, a key indicator of cytotoxicity and apoptosis, in MDA-MB-231 cells treated with

free berberine (BBR), Blank-Lipo, BBR-Lipo, and FA-Lipo. As presented in Fig. 10(a), FA-Lipo treatment resulted in the highest LDH release (693.41 ± 42.7 nmol/mg protein), significantly greater than BBR-Lipo (541.82 ± 36.9 nmol/mg), free BBR (489.63 ± 28.4 nmol/mg), and Blank-Lipo (435.25 ± 25.6 nmol/mg). The elevated LDH release with FA-Lipo indicates extensive membrane damage and loss of cellular integrity, in agreement with its superior cytotoxicity and apoptotic response demonstrated in previous assays.

The LDH release pattern followed FA-Lipo > BBR-Lipo > Free BBR ≫ Blank-Lipo, demonstrating a direct relationship between intracellular berberine accumulation and membrane destabilization. FA functionalization markedly enhanced receptor-mediated uptake in FR-overexpressing TNBC cells, resulting in higher intracellular drug levels and stronger oxidative burden. The amplified oxidative and mitochondrial stress induced by FA-Lipo is consistent with previous observations that folate-decorated nanocarriers promote efficient internalization and mitochondrial localization of phytochemicals, leading to secondary membrane rupture and LDH enzyme leakage. These results confirm that folate-targeted nanoliposomes not only improve intracellular delivery but also intensify terminal apoptotic and necrotic outcomes through oxidative membrane damage (Girigoswami & Girigoswami, 2025; Unida et al., 2022).

3.7.5.2. Nitric Oxide (NO) Assay

Nitric oxide (NO) generation was quantified to evaluate nitro-oxidative stress as an accompanying mechanism of cytotoxicity. As illustrated in Fig. 10(b), FA-Lipo-treated MDA-MB-231 cells showed the highest NO production (72.36 ± 6.8 μM/mg protein), followed by BBR-Lipo (39.21 ± 4.9 μM/mg), free BBR (22.17 ± 2.2 μM/mg), and Blank-Lipo (19.83 ± 3.6 μM/mg). The prominent elevation of NO levels in FA-Lipo-treated cells suggests that targeted delivery of berberine enhances both oxidative and nitrosative stress, which act synergistically to trigger mitochondrial dysfunction and apoptosis.

The observed hierarchy—FA-Lipo > BBR-Lipo > Free BBR ≈ Blank-Lipo—correlates with the oxidative stress trend noted in the DCFDA assay. FA-functionalized nanoliposomes ensured efficient intracellular accumulation of berberine, resulting in the activation of inducible nitric oxide synthase (iNOS) and overproduction of NO, which further contributed to redox imbalance and apoptotic signaling. This outcome reinforces that receptor-targeted nanocarriers

not only improve cellular uptake but also exacerbate nitro-oxidative stress, a known pro-apoptotic mechanism in TNBC cells (Xi et al., 2025).

3.7.5.3. SOD Assay

Superoxide dismutase (SOD) activity was assessed as an indicator of antioxidant defense status in MDA-MB-231 cells. As shown in Fig. 10(c), Blank-Lipo displayed the highest SOD activity (17.21 ± 1.45 ng/mg protein), followed by free BBR (15.86 ± 1.87 ng/mg) and BBR-Lipo (13.48 ± 1.63 ng/mg), whereas FA-Lipo exhibited the lowest SOD activity (9.94 ± 1.21 ng/mg). The pronounced decline in SOD activity following FA-Lipo exposure indicates substantial depletion of the cellular antioxidant defense due to elevated ROS accumulation, confirming enhanced oxidative stress induced by targeted liposomal delivery.

SOD activity inversely correlated with oxidative stress intensity, following the order Blank-Lipo ≥ Free BBR > BBR-Lipo > FA-Lipo. The significant reduction in SOD activity for FA-Lipo-treated cells suggests exhaustion or inactivation of enzymatic antioxidants under excessive ROS pressure. This effect complements the findings of the DCFDA and NO assays, confirming that folate receptor–mediated delivery amplifies intracellular redox imbalance. Similar observations were reported by Leekha et al. (2019), where drug-loaded nanocarriers caused marked suppression of antioxidant enzymes due to oxidative overburden. Collectively, these results substantiate that FA-functionalized nanoliposomes exert their anticancer efficacy through oxidative stress amplification, mitochondrial injury, and antioxidant depletion.

3.7.5.4. GSH Assay

Reduced glutathione (GSH), a central intracellular antioxidant, plays a crucial role in maintaining redox homeostasis and regulating apoptosis. In control cells, GSH levels were 54.12 ± 7.89 nM/mg/min, closely similar to Blank-Lipo (53.54 ± 5.67 nM/mg/min) and free BBR (51.23 ± 5.39 nM/mg/min) groups. However, a pronounced decrease was observed in BBR-Lipo-treated cells (42.68 ± 7.65 nM/mg/min), with a further decline in FA-Lipo-treated cells (38.76 ± 10.43 nM/mg/min) [Fig. 10(d)]. The significant GSH depletion in FA-Lipo-treated cells reflects severe oxidative stress and correlates with the elevated ROS and NO levels observed earlier. Such reduction arises from the excessive consumption of GSH for neutralizing reactive oxygen and nitrogen species and its conjugation via phase II detoxification pathways, leading to an imbalance between GSH synthesis and utilization.

The order of GSH depletion followed Control > Free BBR > BBR-Lipo > FA-Lipo, confirming that FA-functionalized liposomes induce the most intense oxidative stress. The targeted delivery facilitates higher intracellular berberine accumulation, triggering sustained ROS generation and rapid exhaustion of antioxidant reserves. This loss of GSH compromises the cell's redox buffering capacity, making it more susceptible to oxidative damage and apoptosis. The results are in line with previous findings where folate-decorated nanocarriers significantly reduced GSH levels in FR-positive cancer cells due to enhanced redox cycling and mitochondrial dysfunction (Li et al., 2023; Huang et al., 2022).

3.7.5.5. GST Assay

Glutathione-S-transferase (GST) is a key phase II detoxification enzyme that catalyzes the conjugation of reduced GSH with electrophilic species to neutralize toxic metabolites (66). As shown in Fig. 10(e), control cells exhibited the highest GST activity (67.76 ± 23.61 nM/mg/min), with similar values for Blank-Lipo (65.24 ± 18.72 nM/mg/min) and free BBR (58.41 ± 15.68 nM/mg/min). In contrast, BBR-Lipo treatment resulted in a moderate reduction (49.86 ± 12.74 nM/mg/min), while FA-Lipo showed the lowest GST activity (38.27 ± 9.48 nM/mg/min). The observed decrease in GST activity, especially in FA-Lipo-treated cells, suggests enzyme inactivation and substrate depletion under elevated oxidative stress conditions, where excessive ROS and lipid peroxidation by-products compromise enzymatic thiol groups and reduce catalytic efficiency.

GST activity followed the pattern Control ≥ Free BBR > BBR-Lipo > FA-Lipo, which inversely correlates with oxidative stress severity. The lowest GST activity in FA-Lipo-treated cells indicates enzyme inhibition and depletion of available GSH cofactor due to sustained redox overload. Although GST can initially be upregulated under mild oxidative conditions, prolonged exposure to excessive ROS and NO—as induced by targeted berberine delivery—leads to loss of enzymatic activity and redox collapse. These findings align with reports by Leekha et al. (2019), who demonstrated that strong oxidative insults by drug-loaded nanocarriers downregulated GST and depleted GSH, ultimately triggering apoptosis via redox imbalance. Collectively, the data confirm that FA-functionalized nanoliposomes amplify nitro-oxidative stress beyond the cellular antioxidant threshold, culminating in oxidative damage and apoptotic cell death.

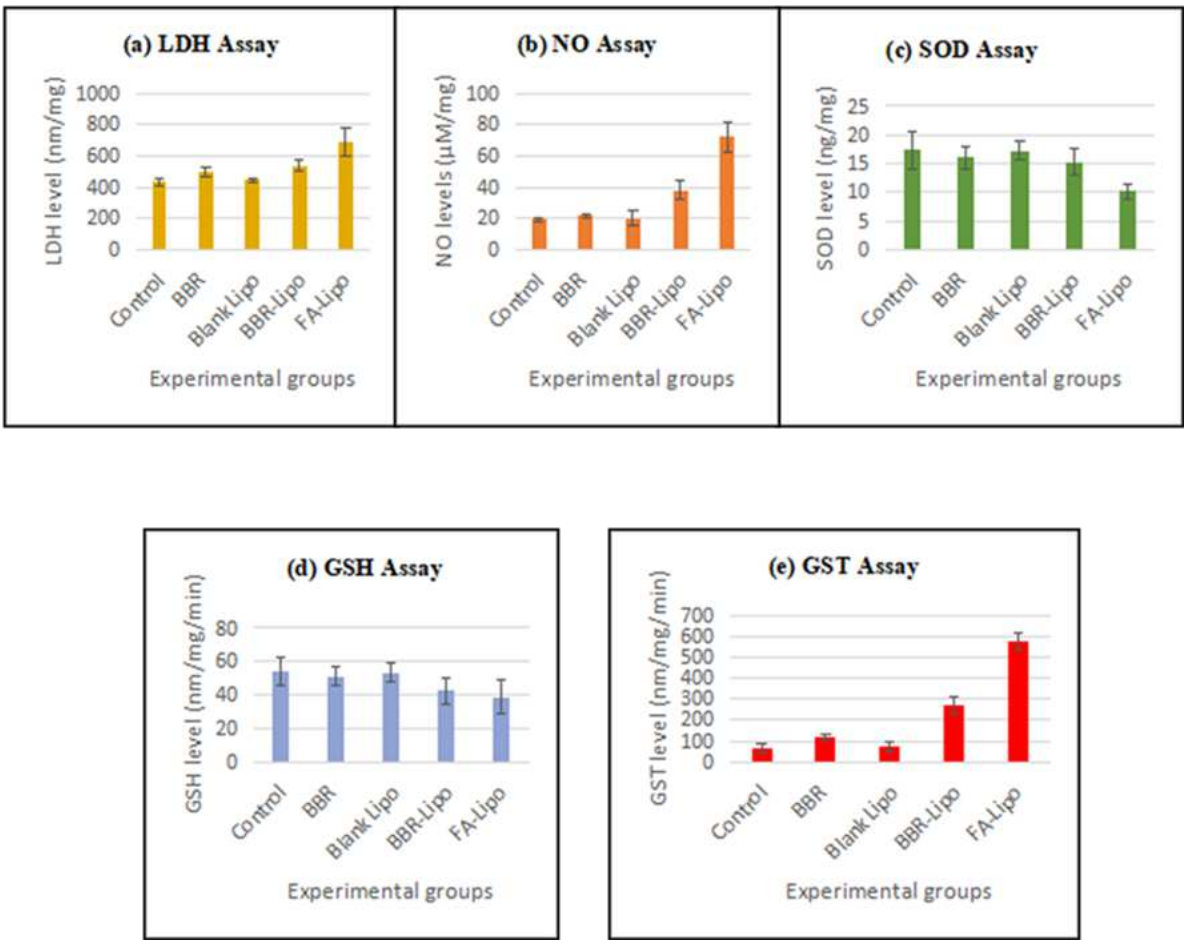


Fig. 10. Plots depicting variations in the levels of (a) LDH, (b) NO, (c) SOD, (d) GSH, and (e) GST in the control and MDA-MB-231 cells treated with BBR, Blank Lipo, BBR-Lipo and FA-Lipo

3.8. Genotoxicity Studies

3.8.1. DAPI Staining of Larval Gut

Following oral administration, the nanoliposomes traversed the Drosophila larval digestive tract and interacted with intestinal epithelial cells. DAPI staining was performed to assess nuclear morphology and detect possible DNA damage. As shown in [Fig. 11(a–b)], the nuclei in control, BBR-Lipo, and FA-Lipo–treated groups (5, 10, and 25 µg/mL) exhibited uniform fluorescence intensity and retained their typical spherical morphology, with no evidence of chromatin condensation, nuclear fragmentation, or apoptotic blebbing. The absence of micronuclei or irregular staining patterns indicates that neither formulation induced genotoxic alterations at the tested concentrations. These findings confirm that the nanoliposomes maintain genomic stability and do not cause nuclear injury in intestinal epithelial cells.

The DAPI results demonstrate that both BBR-Lipo and FA-Lipo were non-genotoxic to larval intestinal tissues within the therapeutic dose range. This observation suggests that the QbD-engineered liposomal systems, although potent in inducing ROS and apoptosis in cancer cells, remain biocompatible toward normal epithelial tissue at equivalent or lower exposures. The lipid components, being biodegradable phospholipids, likely shield berberine from direct contact with nuclear DNA, thereby minimizing oxidative DNA damage. These results are consistent with previous reports where folate-functionalized or phytochemical-loaded nanocarriers exhibited selective cytotoxicity to tumor cells while sparing normal tissues (Chen et al., 2023; Huang et al., 2022).

3.8.2. Trypan Blue Staining

The trypan blue exclusion assay was used to assess the viability of gut epithelial cells after dietary exposure to nanoliposomes. As shown in [Fig. 11(c)], no blue-stained (non-viable) cells were detected in larvae treated with BBR-Lipo or FA-Lipo at concentrations of 5, 10, and 25 µg/mL. The gut epithelium remained intact and morphologically comparable to the untreated control group, indicating that both formulations did not compromise cellular membrane integrity or viability.

The trypan blue results further confirm the non-cytotoxic and biocompatible nature of the liposomal systems toward normal larval gut cells. Despite their strong anticancer activity in TNBC cell lines, these nanoliposomes exhibited minimal off-target toxicity in vivo, demonstrating favorable safety at the gastrointestinal interface. The lipid bilayer encapsulation effectively limits uncontrolled berberine release, preventing nonspecific membrane disruption. Together with the DAPI staining outcomes, these findings highlight that the developed FA-functionalized nanoliposomes possess a high therapeutic index, combining selective tumor cytotoxicity with intestinal safety, thereby supporting their suitability for further translational development.

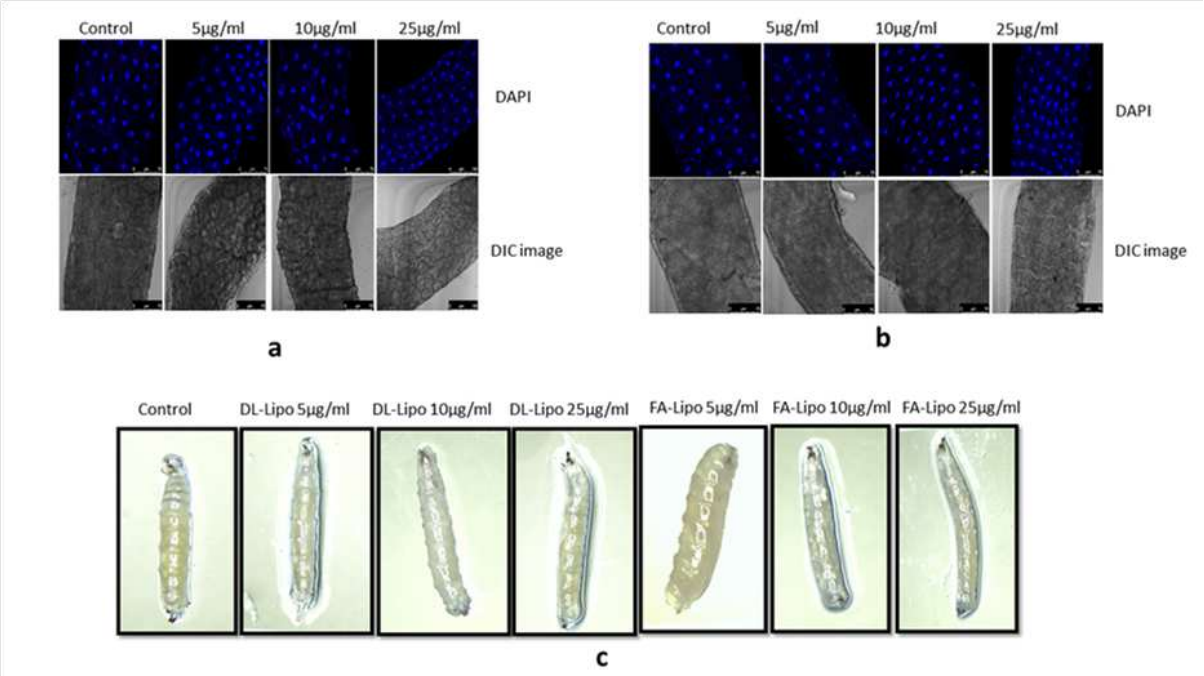


Figure 11: DAPI Fig. 11. DAPI staining of gut (a) BBR-Lipo and (b) FA-Lipo (c) Trypan blue negative

4. Conclusion

Folic acid-functionalized berberine-loaded nanoliposomes (FA-Lipo) were successfully engineered and optimized through a Quality by Design framework using Central Composite Design. The optimized formulation exhibited a nanometric size (~168 nm), high entrapment efficiency (~42%), and excellent physical stability, with a clear shift in zeta potential and uniform spherical morphology confirming effective folate surface functionalization. In vitro studies established that FA-Lipo significantly enhanced therapeutic performance against MDA-MB-231 TNBC cells. Folate decoration markedly increased cellular uptake via receptor-mediated endocytosis, resulting in a ~4.8-fold reduction in IC_{50} compared to free berberine. This translated into pronounced pro-apoptotic effects, evidenced by elevated early and late apoptotic populations, stronger mitochondrial depolarization, and substantial induction of oxidative and nitrosative stress. Elevated ROS and NO, together with depletion of cellular antioxidant defenses (SOD, GSH, GST), highlighted disruption of redox homeostasis as a dominant mechanism contributing to cell death.

The formulation further demonstrated sustained berberine release over 72 hours, supporting prolonged intracellular exposure and continuous pharmacodynamic action. Importantly, genotoxicity analysis in Drosophila larvae revealed minimal DNA damage and no toxicity to normal gut tissues, underscoring the safety of the formulation for non-cancerous systems. Overall, FA-Lipo combines selective receptor-mediated targeting, sustained drug release, and robust apoptotic efficiency with an excellent safety profile. These findings position FA-Lipo as a promising nanotherapeutic platform for TNBC, offering improved efficacy over free drug and non-functionalized liposomes, and warranting further preclinical evaluation, including in vivo tumor models and pharmacokinetic studies for translational advancement.

Statements & Declarations

Funding: No funds, grants, or other support were received during the preparation of this manuscript.

Competing Interests: No relevant financial or non-financial interests to disclose.

Declaration of conflict of interest: The authors declare no conflicts of interest.

Author Contributions:

Roshni Singh: Conceptualization, Methodology, Investigation, Data curation, Formal analysis, Writing – original draft; **Debopriya Dutta:** Writing – review & editing; **Namrata Gautam:** Data curation, Software, Formal analysis, Proofreading; **Meenakshi Tanwar:** Writing – review & editing; **Karishma Niveria:** Investigation; **Disha Mittal:** Writing – review & editing; **Anita Kamra Verma:** Resources, Investigation, Writing – review & editing, Proofreading; **Surajita Sahu:** Investigation; **Monalisa Mishra:** Resources, Investigation; **Saurabh Mittal:** Supervision, Writing – review & editing; **Sushama Talegaonkar:** Conceptualization, Supervision, Writing – review & editing, Project administration.

Data Availability: Not Applicable

Ethics approval: Not Applicable

Clinical trial number: Not Applicable

Consent to participate: Not Applicable

Consent to publish: Not Applicable

References

Ahmadi, M., A. Ritter, C., Woedtke, T. von, Bekeschus, S., & Wende, K. (2024). *Package delivered: Folate receptor-mediated transporters in cancer therapy and diagnosis*. https://doi.org/10.1039/D3SC05539F

Ahmed, S., Gull, A., Alam, M., Aqil, Mohd., & Sultana, Y. (2018). Ultrasonically tailored, chemically engineered and "QbD" enabled fabrication of agomelatine nanoemulsion; optimization, characterization, ex-vivo permeation and stability study. *Ultrasonics Sonochemistry*, *41*, 213–226. https://doi.org/10.1016/j.ultsonch.2017.09.042

Ai, X., Yu, P., Peng, L., Luo, L., Liu, J., Li, S., Lai, X., Luan, F., & Meng, X. (2021). Berberine: A Review of its Pharmacokinetics Properties and Therapeutic Potentials in Diverse Vascular Diseases. *Frontiers in Pharmacology*, *12*, 762654. https://doi.org/10.3389/fphar.2021.762654

Alshaer, W., Nsairat, H., Lafi, Z., Hourani, O. M., Al-Kadash, A., Esawi, E., & Alkilany, A. M. (2023). Quality by Design Approach in Liposomal Formulations: Robust Product Development. *Molecules*, *28*(1), 10. https://doi.org/10.3390/molecules28010010

Alshehade, S. A., Almoustafa, H. A., Alshawsh, M. A., & Chik, Z. (2024). Flow cytometry-based quantitative analysis of cellular protein expression in apoptosis subpopulations: A protocol. *Heliyon*, *10*(13), e33665. https://doi.org/10.1016/j.heliyon.2024.e33665

Ansari, K. A., Vavia, P. R., Trotta, F., & Cavalli, R. (2011). Cyclodextrin-based nanosponges for delivery of resveratrol: In vitro characterisation, stability, cytotoxicity and permeation study. *AAPS PharmSciTech*, *12*(1), 279–286. https://doi.org/10.1208/s12249-011-9584-3

945 Asghari, P., Babaei, A., Zamanian, N., & Eshtivani, E. N.-. (2025). Berberine's impact on health:
946 Comprehensive biological, pharmacological, and nutritional perspectives. *Metabolism*
947 *Open*, *28*, 100399. https://doi.org/10.1016/j.metop.2025.100399
948 Ashhar, M. U., Kumar, S., Ali, J., & Baboota, S. (2021). CCRD based development of
949 bromocriptine and glutathione nanoemulsion tailored ultrasonically for the combined
950 anti-parkinson effect. *Chemistry and Physics of Lipids*, *235*, 105035.
951 https://doi.org/10.1016/j.chemphyslip.2020.105035
952 Atabakhshi-Kashi, M., Carril, M., Mahdavi, H., Parak, W. J., Carrillo-Carrion, C., & Khajeh, K.
953 (2021). In Vitro Cellular Uptake Studies of Self-Assembled Fluorinated Nanoparticles
954 Labelled with Antibodies. *Nanomaterials*, *11*(8), 1906.
955 https://doi.org/10.3390/nano11081906
956 Bellotti, E., Cascone, M. G., Barbani, N., Rossin, D., Rastaldo, R., Giachino, C., & Cristallini, C.
957 (2021). Targeting Cancer Cells Overexpressing Folate Receptors with New Terpolymer-
958 Based Nanocapsules: Toward a Novel Targeted DNA Delivery System for Cancer
959 Therapy. *Biomedicines*, *9*(9), 1275. https://doi.org/10.3390/biomedicines9091275
960 Ben-Fadhel, Y., Maherani, B., Salmieri, S., & Lacroix, M. (2022). Preparation and characterization
961 of natural extracts-loaded food grade nanoliposomes. *LWT*, *154*, 112781.
962 https://doi.org/10.1016/j.lwt.2021.112781
963 Bennett, L. L. (2025). Effects of Pharmacological Dose of Vitamin C on MDA-MB-231 Cells.
964 *Biomedicines*, *13*(3), 640. https://doi.org/10.3390/biomedicines13030640
965 Bian, X., Guo, T., Chen, G., Nie, D., Yue, M., Zhu, Y., & Lin, M. (2024). The therapeutic effect and
966 MR molecular imaging of FA-PEG-FePt/DDP nanoliposomes in AMF on ovarian cancer.
967 *International Journal of Nanomedicine*, *19*, 5227–5243.
968 https://doi.org/10.2147/IJN.S453601

969 Čapek, J., & Roušar, T. (2021). Detection of Oxidative Stress Induced by Nanomaterials in Cells—
970 The Roles of Reactive Oxygen Species and Glutathione. *Molecules*, *26*(16), 4710.
971 https://doi.org/10.3390/molecules26164710
972 Carmona, E. R., Escobar, B., Vales, G., & Marcos, R. (2015). Genotoxic testing of titanium dioxide
973 anatase nanoparticles using the wing-spot test and the comet assay in Drosophila.
974 *Mutation Research. Genetic Toxicology and Environmental Mutagenesis*, *778*, 12–21.
975 https://doi.org/10.1016/j.mrgentox.2014.12.004
976 Eapen, J. V., George, P., Thomas, S., & Antony, J. (2025). Integrative strategies in breast cancer
977 therapy: Conventional approaches, emerging advances, and future challenges. *ASPET*
978 *Discovery*, *1*, 100012. https://doi.org/10.1016/j.aspetd.2025.100012
979 Eruslanov, E., & Kusmartsev, S. (2010). Identification of ROS using oxidized DCFDA and flow-
980 cytometry. *Methods in Molecular Biology (Clifton, N.J.)*, *594*, 57–72.
981 https://doi.org/10.1007/978-1-60761-411-1_4
982 Fan, K.-Q., Zhang, L., Song, F., Zhang, Y.-H., Chen, T., Cheng, X., Su, N., Zou, Y., Yu, T., Tan, F., Xu,
983 W., & Yan, Z. (2025). Pharmacological properties and therapeutic potential of
984 berberine: A comprehensive review. *Frontiers in Pharmacology*, *16*, 1604071.
985 https://doi.org/10.3389/fphar.2025.1604071
986 Freyer, D., & Harms, C. (2017). Kinetic Lactate Dehydrogenase Assay for Detection of Cell
987 Damage in Primary Neuronal Cell Cultures. *Bio-Protocol*, *7*(11), e2308.
988 https://doi.org/10.21769/BioProtoc.2308
989 Geethakumari, D., Bhaskaran Sathyabhama, A., Raji Sathyan, K., Mohandas, D., Somasekharan,
990 J. V., & Thavarool Puthiyedathu, S. (2022). Folate functionalized chitosan nanoparticles
991 as targeted delivery systems for improved anticancer efficiency of cytarabine in MCF-7
992 human breast cancer cell lines. *International Journal of Biological Macromolecules*, *199*,
993 150–161. https://doi.org/10.1016/j.ijbiomac.2021.12.070

994 Girigoswami, K., & Girigoswami, A. (2025). Breast Cancer Progression and Its Theranostic
995 Management via Folate-Directed Targeting of Glycoprotein Receptor. *Medical Sciences*,
996 *13*(4), 275. https://doi.org/10.3390/medsci13040275
997 Gong, J., Wang, H.-X., & Leong, K. W. (2019). Determination of Cellular Uptake and Endocytic
998 Pathways. *Bio-Protocol*, *9*(4), e3169. https://doi.org/10.21769/BioProtoc.3169
999 Gusti, A. M. T., Qusti, S. Y., Alshammari, E. M., Toraih, E. A., & Fawzy, M. S. (2021). Antioxidants-
1000 Related Superoxide Dismutase (SOD), Catalase (CAT), Glutathione Peroxidase (GPX),
1001 Glutathione-S-Transferase (GST), and Nitric Oxide Synthase (NOS) Gene Variants
1002 Analysis in an Obese Population: A Preliminary Case-Control Study. *Antioxidants*, *10*(4),
1003 595. https://doi.org/10.3390/antiox10040595
1004 Hood, R. R., Shao, C., Omiatek, D. M., Vreeland, W. N., & DeVoe, D. L. (2013). Microfluidic
1005 Synthesis of PEG- and Folate-Conjugated Liposomes for One-Step Formation of
1006 Targeted Stealth Nanocarriers. *Pharmaceutical Research*, *30*(6), 1597–1607.
1007 https://doi.org/10.1007/s11095-013-0998-3
1008 Hou, D., Xu, G., Zhang, C., Li, B., Qin, J., Hao, X., Liu, Q., Zhang, X., Liu, J., Wei, J., Gong, Y., Liu, Z.,
1009 & Shao, C. (2017). Berberine induces oxidative DNA damage and impairs homologous
1010 recombination repair in ovarian cancer cells to confer increased sensitivity to PARP
1011 inhibition. *Cell Death & Disease*, *8*(10), e3070–e3070.
1012 https://doi.org/10.1038/cddis.2017.471
1013 Hu, H., Song, Q., Yang, W., Zeng, Q., Liang, Z., Liu, W., Shao, Z., Zhang, Y., Chen, C., & Wang, B.
1014 (2023). Oxidative stress induced by berberine-based mitochondria-targeted low
1015 temperature photothermal therapy. *Frontiers in Chemistry*, *11*, 1114434.
1016 https://doi.org/10.3389/fchem.2023.1114434
1017 Huang, F.-Y. J., Chen, W.-J., Lee, W.-Y., Lo, S.-T., Lee, T.-W., & Lo, J.-M. (2013). In Vitro and in
1018 Vivo Evaluation of Lactoferrin-Conjugated Liposomes as a Novel Carrier to Improve the

Brain Delivery. *International Journal of Molecular Sciences*, *14*(2), 2862–2874. https://doi.org/10.3390/ijms14022862

Ibrahim, M. A. I., Othman, R., Chee, C. F., & Ahmad Fisol, F. (2023). Evaluation of Folate-Functionalized Nanoparticle Drug Delivery Systems—Effectiveness and Concerns. *Biomedicines*, *11*(7), 2080. https://doi.org/10.3390/biomedicines11072080

Jain, A., & Jain, S. (2016). In vitro release kinetics model fitting of liposomes: An insight. *Chemistry and Physics of Lipids*, *201*. https://doi.org/10.1016/j.chemphyslip.2016.10.005

Karpuz, M., Gundogdu, E., Demir, E., & Senyigit, Z. (2021). Radiolabeled Tedizolid Phosphate Liposomes for Topical Application: Design, Characterization, and Evaluation of Cellular Binding Capacity. *AAPS PharmSciTech*, *22*. https://doi.org/10.1208/s12249-020-01917-4

Kashyap, A., Umar, S. M., Dev J.R., A., Mendiratta, M., & Prasad, C. P. (2022). In vitro anticancer efficacy of a polyphenolic combination of Quercetin, Curcumin, and Berberine in triple negative breast cancer (TNBC) cells. *Phytomedicine Plus*, *2*(2), 100265. https://doi.org/10.1016/j.phyplu.2022.100265

Katerji, M., Filippova, M., & Duerksen-Hughes, P. (2019). Approaches and Methods to Measure Oxidative Stress in Clinical Samples: Research Applications in the Cancer Field. *Oxidative Medicine and Cellular Longevity*, *2019*, 1279250. https://doi.org/10.1155/2019/1279250

Kim, E.-S. (2025). Molecular targets and therapies associated with poor prognosis of triple-negative breast cancer (Review). *International Journal of Oncology*, *66*(6), 52. https://doi.org/10.3892/ijo.2025.5758

Kotouček, J., Hubatka, F., Mašek, J., Kulich, P., Velínská, K., Bezděková, J., Fojtíková, M., Bartheldyová, E., Tomečková, A., Stráská, J., Hrebík, D., Macaulay, S., Kratochvílová, I., Raška, M., & Turánek, J. (2020). Preparation of nanoliposomes by microfluidic mixing in

herring-bone channel and the role of membrane fluidity in liposomes formation. *Scientific Reports*, *10*(1), 5595. https://doi.org/10.1038/s41598-020-62500-2

Kumar, P., Huo, P., & Liu, B. (2019). Formulation Strategies for Folate-Targeted Liposomes and Their Biomedical Applications. *Pharmaceutics*, *11*(8), 381. https://doi.org/10.3390/pharmaceutics11080381

Lakshmanan, I., & Batra, S. K. (2013). Protocol for Apoptosis Assay by Flow Cytometry Using Annexin V Staining Method. *Bio-Protocol*, *3*(6), e374. https://doi.org/10.21769/bioprotoc.374

Lasic, D. D. (1988). The mechanism of vesicle formation. *Biochemical Journal*, *256*(1), 1–11. https://doi.org/10.1042/bj2560001

Li, W., Liu, Y., Wang, B., Luo, Y., Hu, N., Chen, D., Zhang, X., & Xiong, Y. (2016). Protective effect of berberine against oxidative stress-induced apoptosis in rat bone marrow-derived mesenchymal stem cells. *Experimental and Therapeutic Medicine*, *12*(6), 4041–4048. https://doi.org/10.3892/etm.2016.3866

Liu, D., Meng, X., Wu, D., Qiu, Z., & Luo, H. (2019). A Natural Isoquinoline Alkaloid With Antitumor Activity: Studies of the Biological Activities of Berberine. *Frontiers in Pharmacology*, *10*, 9. https://doi.org/10.3389/fphar.2019.00009

Majumdar, S., Mahanti, B., Kar, A. K., Parya, H., Ghosh, A., & Kar, B. (2024). Nanoliposome: As a smart nanocarrier in transdermal drug delivery system. *Intelligent Pharmacy*, *2*(6), 768–776. https://doi.org/10.1016/j.ipha.2024.04.004

Marshalek, J. P., Sheeran, P. S., Ingram, P., Dayton, P. A., Witte, R. S., & Matsunaga, T. O. (2016). Intracellular delivery and ultrasonic activation of folate receptor-targeted phase-change contrast agents in breast cancer cells in vitro. *Journal of Controlled Release : Official Journal of the Controlled Release Society*, *243*, 69–77. https://doi.org/10.1016/j.jconrel.2016.09.010

Mittal, S., Ali, J., & Baboota, S. (2021). Enhanced anti-psoriatic activity of tacrolimus loaded nanoemulsion gel via omega 3—Fatty acid (EPA and DHA) rich oils-fish oil and linseed oil. *Journal of Drug Delivery Science and Technology*, *63*, 102458. https://doi.org/10.1016/j.jddst.2021.102458

Mittal, S., Ali, J., & Baboota, S. (2022). DoE Engineered Development and Validation of an RP-HPLC Method for Simultaneous Estimation of Temozolomide and Resveratrol in Nanostructured Lipid Carrier. *Journal of AOAC INTERNATIONAL*, qsac045. https://doi.org/10.1093/jaoacint/qsac045

Mittal, S., Shah, S., Yadav, H. N., Ali, J., Gupta, M. M., & Baboota, S. (2023). Quality by design engineered, enhanced anticancer activity of temozolomide and resveratrol coloaded NLC and brain targeting via lactoferrin conjugation in treatment of glioblastoma. *European Journal of Pharmaceutics and Biopharmaceutics: Official Journal of Arbeitsgemeinschaft Fur Pharmazeutische Verfahrenstechnik e.V*, *191*, 175–188. https://doi.org/10.1016/j.ejpb.2023.08.018

Moloudi, K., Abrahamse, H., & George, B. P. (2024). Application of liposomal nanoparticles of berberine in photodynamic therapy of A549 lung cancer spheroids. *Biochemistry and Biophysics Reports*, *40*, 101877. https://doi.org/10.1016/j.bbrep.2024.101877

Nair, A., Singh, R., Gautam, N., Saxena, S., Mittal, S., Shah, S., & Talegaonkar, S. (2024). Multifaceted role of phytoconstituents based nano drug delivery systems in combating TNBC: A paradigm shift from chemical to natural. *Naunyn-Schmiedeberg's Archives of Pharmacology*, *397*(12), 9207–9226. https://doi.org/10.1007/s00210-024-03234-0

Namjoshi, S., Dabbaghi, M., Roberts, M. S., Grice, J. E., & Mohammed, Y. (2020). Quality by Design: Development of the Quality Target Product Profile (QTPP) for Semisolid Topical Products. *Pharmaceutics*, *12*(3), 287. https://doi.org/10.3390/pharmaceutics12030287

Nguyen-Huu, A.-M., Le, N. T. T., Vo Do, M. H., Dong Yen, P. N., Nguyen-Dinh, T.-D., Nguyen, N. H., & Nguyen, D. H. (2024). Development and Characterization of Quercetin-Loaded

Polymeric Liposomes with Gelatin-Poly(ethylene glycol)-Folic Acid Coating to Increase Their Long-Circulating and Anticancer Activity. *ACS Applied Bio Materials*, *7*(7), 4454–4470. https://doi.org/10.1021/acsabm.4c00334

Parvathaneni, V., Shukla, S. K., & Gupta, V. (2023). Development and Characterization of Folic Acid-Conjugated Amodiaquine-Loaded Nanoparticles–Efficacy in Cancer Treatment. *Pharmaceutics*, *15*(3), Article 3. https://doi.org/10.3390/pharmaceutics15031001

Patel, P., Raval, M., Airao, V., Ali, N., Shazly, G. A., Khan, R., & Prajapati, B. (2024). Formulation of Folate Receptor-Targeted Silibinin-Loaded Inhalable Chitosan Nanoparticles by the QbD Approach for Lung Cancer Targeted Delivery. *ACS Omega*, *9*(9), 10353–10370. https://doi.org/10.1021/acsomega.3c07954

Pathak, S., Singh, R., Hussain, A., Siddiqui, N. A., Mittal, S., & Gupta, A. (2024). QbD Approach for the Development of Tea Tree Oil-Enhanced Microemulgel Loaded with Curcumin and Diclofenac for Rheumatoid Arthritis Treatment. *Gels*, *10*(10), 634. https://doi.org/10.3390/gels10100634

Pramod, K., Tahir, M. A., Charoo, N. A., Ansari, S. H., & Ali, J. (2016). Pharmaceutical product development: A quality by design approach. *International Journal of Pharmaceutical Investigation*, *6*(3), 129–138. https://doi.org/10.4103/2230-973X.187350

Ramana, L. N., Sethuraman, S., Ranga, U., & Krishnan, U. M. (2010). Development of a liposomal nanodelivery system for nevirapine. *Journal of Biomedical Science*, *17*(1), 57. https://doi.org/10.1186/1423-0127-17-57

Rauf, A., Abu-Izneid, T., Khalil, A. A., Imran, M., Shah, Z. A., Emran, T. B., Mitra, S., Khan, Z., Alhumaydhi, F. A., Aljohani, A. S. M., Khan, I., Rahman, Md. M., Jeandet, P., & Gondal, T. A. (2021). Berberine as a Potential Anticancer Agent: A Comprehensive Review. *Molecules*, *26*(23), 7368. https://doi.org/10.3390/molecules26237368

Redza-Dutordoir, M., & Averill-Bates, D. A. (2016). Activation of apoptosis signalling pathways by reactive oxygen species. *Biochimica et Biophysica Acta (BBA) - Molecular Cell Research*, *1863*(12), 2977–2992. https://doi.org/10.1016/j.bbamcr.2016.09.012

Rhee, I., Ahmad, T., Hong, S., Chang, Y., & Lee, J. (2010). Silica-coated Iron-oxide Nanoparticles Synthesized as a T_2 Contrast Agent for Magnetic Resonance Imaging by Using the Reverse Micelle Method. *Journal of The Korean Physical Society - J KOREAN PHYS SOC*, *57*. https://doi.org/10.3938/jkps.57.1545

Rostami, N., Gomari, M. M., Abdouss, M., Moeinzadeh, A., Choupani, E., Davarnejad, R., Heidari, R., & Bencherif, S. A. (2023). Synthesis and Characterization of Folic Acid-Functionalized DPLA-co-PEG Nanomicelles for the Targeted Delivery of Letrozole. *ACS Applied Bio Materials*, *6*(5), 1806–1815. https://doi.org/10.1021/acsabm.3c00041

Rudzińska, M., Grygier, A., Knight, G., & Kmiecik, D. (2024). Liposomes as Carriers of Bioactive Compounds in Human Nutrition. *Foods*, *13*(12), 1814. https://doi.org/10.3390/foods13121814

Saberian, E., Jenčová, J., Jenča, A., Salehipoor, F., Zare-Zardini, H., Petrášová, A., Džupa, P., Ebrahimifar, M., Allahyartorkaman, M., & Jenča, J. (2025). Bleomycin-loaded folic acid-conjugated nanoliposomes: A novel formulation for targeted treatment of oral cancer. *Frontiers in Bioengineering and Biotechnology*, *13*. https://doi.org/10.3389/fbioe.2025.1535793

Sabit, H., Adel, A., Abdelfattah, M. M., Ramadan, R. M., Nazih, M., Abdel-Ghany, S., El-hashash, A., & Arneth, B. (2025). The role of tumor microenvironment and immune cell crosstalk in triple-negative breast cancer (TNBC): Emerging therapeutic opportunities. *Cancer Letters*, *628*, 217865. https://doi.org/10.1016/j.canlet.2025.217865

Schieber, M., & Chandel, N. S. (2014). ROS Function in Redox Signaling and Oxidative Stress. *Current Biology : CB*, *24*(10), R453–R462. https://doi.org/10.1016/j.cub.2014.03.034

Shrivastava, N., Parikh, A., Dewangan, R. P., Biswas, L., Verma, A. K., Mittal, S., Ali, J., Garg, S., & Baboota, S. (2022). Solid Self-Nano Emulsifying Nanoplatform Loaded with Tamoxifen and Resveratrol for Treatment of Breast Cancer. *Pharmaceutics*, *14*(7), Article 7. https://doi.org/10.3390/pharmaceutics14071486

Siddiqui, L., Bag, J., Seetha, Mittal, D., Leekha, A., Mishra, H., Mishra, M., Verma, A. K., Mishra, P. K., Ekielski, A., Iqbal, Z., & Talegaonkar, S. (2020). Assessing the potential of lignin nanoparticles as drug carrier: Synthesis, cytotoxicity and genotoxicity studies. *International Journal of Biological Macromolecules*, *152*, 786–802. https://doi.org/10.1016/j.ijbiomac.2020.02.311

Singh, I., Swami, R., Pooja, D., Jeengar, M. K., Khan, W., & Sistla, R. (2016). Lactoferrin bioconjugated solid lipid nanoparticles: A new drug delivery system for potential brain targeting. *Journal of Drug Targeting*, *24*(3), 212–223. https://doi.org/10.3109/1061186X.2015.1068320

Su, L.-J., Zhang, J.-H., Gomez, H., Murugan, R., Hong, X., Xu, D., Jiang, F., & Peng, Z.-Y. (2019). Reactive Oxygen Species-Induced Lipid Peroxidation in Apoptosis, Autophagy, and Ferroptosis. *Oxidative Medicine and Cellular Longevity*, *2019*, 5080843. https://doi.org/10.1155/2019/5080843

Sun, J., Chen, X., Liu, T., Jiang, X., Wu, Y., Yang, S., Hua, W., Li, Z., Huang, H., Ruan, X., & Du, X. (2018). Berberine Protects Against Palmitate-Induced Apoptosis in Tubular Epithelial Cells by Promoting Fatty Acid Oxidation. *Medical Science Monitor : International Medical Journal of Experimental and Clinical Research*, *24*, 1484. https://doi.org/10.12659/MSM.908927

Unida, V., Vindigni, G., Raniolo, S., Stolfi, C., Desideri, A., & Biocca, S. (2022). Folate-Functionalization Enhances Cytotoxicity of Multivalent DNA Nanocages on Triple-Negative Breast Cancer Cells. *Pharmaceutics*, *14*(12), 2610. https://doi.org/10.3390/pharmaceutics14122610

Xi, M., Kia, S. H., Shi, H., Dong, X., Shi, Y., Zhang, L., & Jiang, B. (2025). Synthesis and characterization of berberine-loaded nanoliposome for targeting of MAPK pathway to induce apoptosis and suppression of autophagy in glioblastoma. *Biomedical Materials (Bristol, England)*, *20*(2). https://doi.org/10.1088/1748-605X/adb673

Xiong, R.-G., Huang, S.-Y., Wu, S.-X., Zhou, D.-D., Yang, Z.-J., Saimaiti, A., Zhao, C.-N., Shang, A., Zhang, Y.-J., Gan, R.-Y., Li, H.-B., Xiong, R.-G., Huang, S.-Y., Wu, S.-X., Zhou, D.-D., Yang, Z.-J., Saimaiti, A., Zhao, C.-N., Shang, A., … Li, H.-B. (2022). Anticancer Effects and Mechanisms of Berberine from Medicinal Herbs: An Update Review. *Molecules*, *27*(14). https://doi.org/10.3390/molecules27144523

Ye, P., Zhang, W., Yang, T., Lu, Y., Lu, M., Gai, Y., Ma, X., & Xiang, G. (2014). Folate receptor-targeted liposomes enhanced the antitumor potency of imatinib through the combination of active targeting and molecular targeting. *International Journal of Nanomedicine*, *9*, 2167–2178. https://doi.org/10.2147/IJN.S60178

Zhang, M., Liu, J., Yu, C., Tang, S., Jiang, G., Zhang, J., Zhang, H., Xu, J., & Xu, W. (2022). Berberine Regulation of Cellular Oxidative Stress, Apoptosis and Autophagy by Modulation of m6A mRNA Methylation through Targeting the Camk1db/ERK Pathway in Zebrafish-Hepatocytes. *Antioxidants*, *11*(12), 2370. https://doi.org/10.3390/antiox11122370

Zhu, Y., Xie, N., Chai, Y., Nie, Y., Liu, K., Liu, Y., Yang, Y., Su, J., & Zhang, C. (2022). Apoptosis Induction, a Sharp Edge of Berberine to Exert Anti-Cancer Effects, Focus on Breast, Lung, and Liver Cancer. *Frontiers in Pharmacology*, *13*, 803717. https://doi.org/10.3389/fphar.2022.803717